University of Alberta

Biofilm Streamer Formation in a Porous Microfluidic Device

by

Amin Valiei

A thesis submitted to the Faculty of Graduate Studies and Research
in partial fulfilment of the requirements for the degree of

Master of Science

in

Chemical Engineering

Department of Chemical and Materials Engineering

Spring 2013
Edmonton, Alberta

I would like to dedicate my thesis to my parents for their love, encouragement and continuous support

Abstract

Biofilm formation in porous media is of significant importance in many environmental and industrial processes such as bioremediation, oil recovery, and wastewater treatment. Among various environmental cues, hydrodynamic conditions are considered an important determinant of the dynamics of biofilm formation. However, the investigation of biofilm formation dynamics in porous media under different fluidic conditions presents a challenging task due to opacity and complexity of the real porous media systems. In the present study, we fabricated a porous media mimic inside a microfluidic device to observe the growth of bacteria in a porous environment. Using a microfluidic platform enables the precise control of the flow in the length scales comparable to the dimensions of microbes, thus providing reliable tools for characterization of different biofilm structures. Here, we report the formation of filamentous structures between the porous structures following the infusion of bacterial solution. These filamentous structures, which are known as streamers, are viscoelastic materials composed of Extracellular Polymeric Substance (EPS) and are tethered at one or both ends to a surface, while the rest of the structure floats in the aqueous media. We studied evolution of streamers in different flow rates and identified a tangible link between hydrodynamic conditions and development of these filamentous structures. Our results show that hydrodynamic conditions not only play a key role in determining the formation and stability of the streamers, but also influence their morphology and distribution. These observations, which reveal salient features of biofilm formation in porous media, could open

up new avenues for understanding biofilm dynamics in complex natural conditions.

Acknowledgement

First, I would like to express my deepest sense of gratitude to my advisor Professor Thomas Thundat for his continuous support during my M.Sc. study, for his enthusiasm, and immense knowledge. His guidance helped me in all the time of research. I could not have imagined having a better advisor and mentor for my M.Sc. study.

I also would like to express my sincere gratitude to Dr. Aloke Kumar for his absolute support and guidance throughout the entire M.Sc. project and my thesis. He is always available for discussion, and his comments are always insightful. He sets a model example for me by his enthusiasm and persistence toward research and life.

I would like to greatly thank my defence committee Prof. Yang Liu and Prof. Nede Nazemifard for their useful suggestions. I thank Prof. Liu for making her lab facilities available to me. It was an enjoyable time to learn from graduate students in her lab especially Xiaohui Sun and Toa Dong. They answered my many questions and helped me to get this research going.

I would like to thank Professor Subir Bhattacharjee for his useful inputs and his help in making the facilities at OSCIEF available to me. I am also grateful to Ni Yang for helping me in using the image facilities at OSCIEF.

I would also like to thank all the personnel at Micro and Nanofabrication Facility at the University of Alberta for their assistance in using various facilities and providing useful suggestions.

I would like to thank Professor Howard Ceri from the Department of Biological Science of the University of Calgary for providing bacterial strains for this research.

I would like to thank all my group mates at Nano Interface and Molecular Engineering group at the University of Alberta. I learned a great deal from them and had an enjoyable time working and interacting with them.

Finally, I would like to thank my parents from the deep of my heart for their support and encouragement during my master's study and whole life. To them, I dedicate my thesis.

Table of Contents

List of Figures

1 Introduction to Biofilms

1.1 Surfaces and bacteria

Biofilms are complex, dynamic and three-dimensional communities of bacteria that form at interfaces such as a solid-liquid interface. Bacteria in biofilms are encased in a self-secreted polymeric substance termed extracellular polymeric substances (EPS) and they exhibit a mode of growth that is distinct from planktonic or free floating bacteria [1]. Although fossil records show that biofilms have existed since ancient times, probably as long as the existence of bacteria themselves, their appreciation as a distinct mode of living has only begun to be understood over the last 50 years [2]. Research in the last few decades suggests that biofilm is not only a distinct mode of living for microbes, it is also the predominant mode of life for the them, forming on a wide variety of abiotic and biotic surfaces such as glass, plastics, metals and even human tissues.

Biofilm formation on surface is a very complex process, and a multitude of events (often concurrent) participate in this phenomenon (Figure 1.1). Attachment events are one of most important aspects of biofilms formation. Bacteria use many organelles such as flagella and pili to sense and attach reversibly to the surfaces (step 1 in Figure 1.1) [3]. The change from the reversible to irreversible attachment begins with the secretion of extracellular matrix (EPS), which is composed of polysaccharides, proteins, and nucleic acids. Presence of sticky EPS mediates the permanent bonding between the cells and surface (step 2). Along with the increasing accumulation of EPS, biofilm structure

propagates with the replication of adhered cells and incorporation of more cells from the bulk fluid leading to the formation of small microcolonies (step 3). These micro colonies grow to form a mature biofilm possessing a three dimensional structure (step 4). The biofilm cycle continues as some cells detach from the mature biofilm and form biofilm communities in new environmental niches (step 5) [4].

The complex transition of bacteria from planktonic to biofilms offers several advantages to the microbes. Research has established that bacteria in biofilms are more resistant to a variety of external stresses as compared to the planktonic bacteria. EPS, which surrounds the bacteria in biofilms, often acts as a barrier to protect the bacteria from antibiotics, mechanical stress, ultraviolet radiation, and host immune system [5]. In addition, many of the bacteria in biofilm are in slow-growing state which makes them less susceptible to antimicrobial agents. Other advantageous features of biofilm formation are communalistic and mutualistic symbiotic relationships and exchange of genetic material resulted from the proximity of bacteria within biofilms [6].

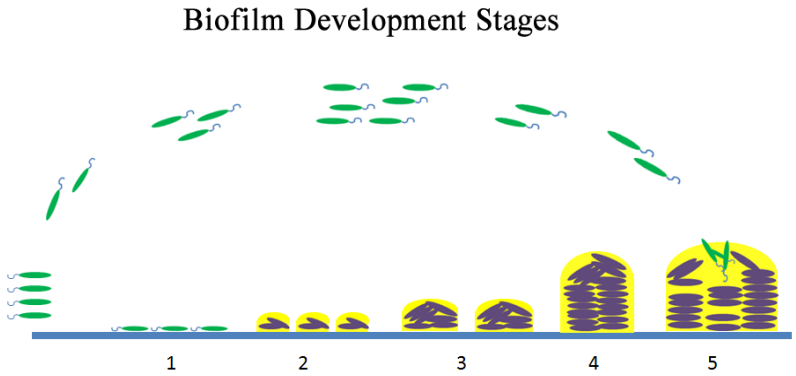

Figure 1.1 Biofilm development stages. Stage 1: reversible attachment of cells to surface. Stage 2: irreversible attachment of bacteria to the surface and EPS formation (yellow). Stage 3: formation of microcolonies. Stage 4: formation of a mature biofilm structure. Stage 5: dispersal of cells from biofilm.

The ability of bacteria to easily attach to surfaces and form biofilms has significant implications in natural, industrial, and clinical settings. In nature, biofilms play a major role in aquatic ecosystems such as lakes and rivers by contributing to energy flows and recycling of nutrients [7]. It is reported that the bacteria that live in biofilm communities are 1000-10000 more than the population of planktonic bacteria in pristine alpine streams [8]. Resistance of biofilms to environmental stresses has caused them to survive in extreme environments from hot desserts to the depth of oceans, to interstices of rocks buried thousands of feet below the earth's surface. It is estimated that biofilms constitute more than half of the biomass and more than 98% of the bacterial species on the planet [9].

In industrial systems, biofilms are responsible for a wide variety of problems. Biofouling inside the pipes reduces the heat transfer efficiency of heat exchangers and causes blocking of pipes in process and power industries. Biofilm formation also induces the corrosion of metals in piping systems and process equipment, a phenomenon known as “biocorrosion”. Release of microbes from the cooling towers, water distribution systems, and food processing equipment poses serious risks to human health [10]. Apart from their detrimental effects, biofilms are also used in many advantageous ways in industry. Metabolic activity of microbial cells in biofilm can be used to degrade contaminants in water and wastewater treatment facilities [11]. A related application is the microbial fuel cell (MFC) [12], where biofilms are used for the generation of electricity from organic matter. Microbial biofilm can

also be employed for the high efficiency extraction of metals from their ores in a process called “bioleaching” [13].

In human body, biofilms have been found to be responsible for a wide variety of infections. It is estimated that bacterial biofilms are involved in at least 60% of the human infections [14]. Examples of biofilm infections of human body include dental plaque, middle air infections, cystic fibrosis, and native valve endocarditis. Biofilms can also form on indwelling medical devices such as catheters, heart valves, as well as artificial veins and joints leading to serious infections. Over half of the two million cases of nosocomial infections in United States are associated with indwelling devices. Once these infections develop they are difficult to treat effectively due to the increased resistance of biofilms to antimicrobial agents and immune defence mechanisms, thus they cause severe economical costs and burdens to the healthcare system.

Given the wide application of biofilms in natural, clinical, and engineered settings, considerable amount of research has been done in order to better understand and control biofilms. Scientists have been able to develop fairly good insight into biofilm formation on simple geometries such as flat surfaces and tubes. However, little is known about biofilm structures in complex geometries. Porous media represent one such situation. The following section discusses the importance of biofilm formation in porous media and explains the approach that we used to study the biofilm formation in porous media.

1.2 **Biofilm formation in porous media**

Porous media provide bacteria with an interesting habitat. Not only do they possess a high specific area, the tortuous pore-structure of porous media can also provide extensive gradients of various physiochemical properties such as pressure, nutrient concentrations and pH. Such complex systems can provide bacteria with a very unique habitat and a very versatile ecological niche. An example of a porous medium is the soil. Physical and chemical consequences of biofilm formation in the soil can play a singularly important role in several subsurface activities including bio-clogging, CO_2 sequestration, water transport, and various chemical cycles (e.g., nitrogen fixation).

Clogging or reduction of porosity and permeability of porous media due to biofilm formation in the pore-spaces is one of the serious physical consequences of bacterial activity in such a complex medium. Biofilm clogging of wellbores poses serious operational problems during the secondary oil recovery operations, where water flooding is performed to enhance the efficiency of oil extraction [15]. Production of copious amounts of EPS during biofilm formation is considered as the main cause of reduction of permeability, particularly when it traps particulate materials from the environment [16]. Clogging ability of biofilms can also be used for profit. For instance, in one technique, nutrients are injected into reservoir to trigger the formation of biofilms in high permeability zones that are mainly occupied by water after the secondary oil recovery operation. In this process, “selective plugging” of high permeability zones by EPS drives the water to low permeability zones. The mobilized water replaces the residual oil and improves

the oil production efficiency. Another example of the beneficial impacts of clogging ability of biofilms is the development of the "biobarrier" technology to limit the spread of contaminants resulting from leaking of underground storage tanks, landfills sites, and chemical or oil spills [17]. In this technology, the ability of biofilms to secrete EPS is used to block the pore spaces resulting in either reduction of groundwater flow through certain areas or redirection of flow to certain locations [18]. Figure 1.2 shows a schematic of a biobarrier designed to restrict the flow of pollutants to the underground water.

Biofilm formation also changes the chemical microenvironment of porous media. Recently, it is demonstrated that the metabolic activity of bacteria within the biobarriers can be effectively used to reduce the concentration of contaminants as well as their spread. The ultimate goal in the design of this novel type of biobarriers, which are called "reactive biobarriers", is to optimize the permeability reduction of the soil resulted from the propagation of biofilms, while the contaminated pollutants are being removed by the metabolic activity of bacteria at the same time. Successful implementation of reactive biobarriers for the treatment of chlorinated solvents, heavy metals and radionucluids have been reported in several field situations [19]. As in the case of biobarriers, porous media biofilms can also be utilized in biofilters for the removal of contaminants in different wastewater and hazardous waste treatment processes [20]. In another application, different metabolism by products of bacteria such as gases, biosurfactants, solvents, and acids are used to modify the interfacial properties of oil-water systems, leading to higher oil

extraction efficiencies in different microbial enhanced oil recovery (MEOR) techniques.

Whether beneficial or detrimental, the widespread implications of chemical and physical effects of porous media biofilms in industry suggest that understanding and controlling the spatial-temporal properties of biofilm in porous media is a necessary task. Several factors influence the biofilm formation process. Cell to cell signalling, motility functions, microbial cell properties, which include size, density and surface properties, as well as secretion of EPS are some of the effective biological parameters that affect the biofilm development [19, 21]. Environmental factors such as hydrodynamics, pH, temperature, and nutrient concentration have also been reported to play an important role in the biofilm formation. While both biological and environmental factors are important in the biofilm formation, easy manipulation of environmental conditions provide a more advantageous way to control the spatial and temporal properties of biofilms for the improvement of the efficiency of the different industrial and environmental processes.

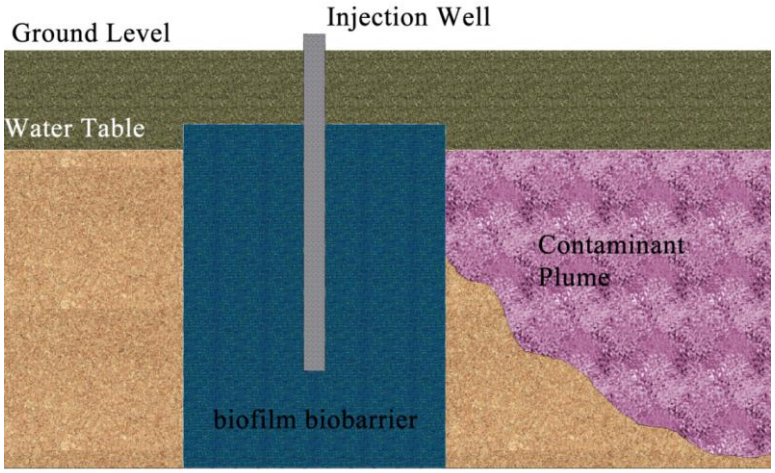

Figure 1.2 A schematic of the biobarrier technology used to inhibit the spreading of contaminants.

Of the various environmental factors that play a significant role in the biofilm formation, hydrodynamics is one of the most important. Hydrodynamics has a profound and complex effect on the temporal and spatial properties of biofilms by determining the transport of different molecules and microbes. Hydrodynamics is known to influence all the stages of biofilm formation. For example, higher flow rates can lead to better nutrient availability for the microbes during the initial stages of biofilm formation. After the formation of a mature biofilm, shear stress can facilitate detachment of microbes and thus allowing microbes to explore fresh locations. Hydrodynamic conditions can also lead to the change in the morphology of biofilms. Biofilm structures can vary from mushroom shape structures to filamentous structures on flat surfaces depending on the flow regime. On the other hand, EPS formation in the pore spaces can lead to wetting instabilities and preferential flow paths.

Due to its importance, the inter-relationship between hydrodynamics and biofilm formation in porous media has been investigated by several researchers [19, 22-25]. Despite these efforts several facets of this inter-relationship remain ill understood. Here, the advent of microfabrication enabled microfluidics to provide researchers with a new opportunity. By recreating the micro-environment of the porous media at small scales (~ μm), microfluidic technology allows real-time studies at multiple temporal and spatial scales.

1.3 Thesis outline

The broad goal of this research is to evolve a fundamental understanding of how biofilms grow in porous media and how external factors influence such growth. To this end, we fabricated porous media mimics and used them as an experimental platform to conduct our study. The remaining portion of the thesis is organized into the following chapters:

Chapter 2: in this chapter, the experimental framework for studying biofilm formation in porous media is explained. We develop a simple two dimensional porous media in a microfluidic chamber and in this chapter, we present an explanation of our experimental setup.

Chapter 3: the results of the experimental examination of biofilm formation in porous media are presented. We discovered that under certain hydrodynamic conditions, biofilm formation inside the porous media proceeded through the formation of filamentous structures known as streamers. We investigated the spatial-temporal properties of streamers under different flow conditions.

Chapter 4: we performed numerical simulation using finite element method to analyse the hydrodynamic conditions in our microfluidic device. Results of the numerical simulation of fluid flow are compared with the experimental data obtained in Chapter 3 to understand the inter-relationship between streamer formation and imposed hydrodynamic conditions.

Chapter 5: in this chapter new possible research directions for understanding biofilm streamers in porous media are proposed.

2 Microfluidic porous media mimics

2.1 Introduction

Microfluidics is the science and technology that deals with the handling and manipulation of fluids in miniaturized channels (with the dimension of tens to hundreds of microns) [26]. Some of the advantages that microfluidic devices provide are: small reagent volumes, fast reaction times, and possibility of parallel and high throughput reactions [27]. Apart from these advantages, one of the distinct features of the fluid flow in microfluidic devices is the change in fundamental physics of the problem due to miniaturization [28]. Fluid Flow regime in microfluidic devices is laminar and it is dominated by surface forces. The unique features of flow in microfluidic devices open new avenues for understanding different micro scale phenomena that cannot be investigated by traditional approaches. Due to these and other unique and interesting characteristics of microfluidic devices, they have triggered important advances in conducting fundamental experiments in biotechnology, materials science, and chemistry [29].

Microfluidic devices are considered powerful tools in biological research with a wide variety of applications, ranging from cell biology to point of care diagnostics, to microbiology [30-32]. One of the most recent advances in microfluidic technology is the application of microfluidic devices in studying microbial biofilms. The use of microfluidic devices offers several advantages for studying biofilms. Microfluidic devices enable the study of the effect of environmental conditions by precise controlling of

microenvironment around the cells. Additionally, most of the biofilm formation related phenomena such as adhesion, cell to cell communication, etc. occur over the length scales which are compatible with the length scale of microfluidic devices. Finally, emergence of novel microfabrication techniques allows the fabrication of different geometrical features and investigation of their effects on biofilm formation [33]. Recent studies have demonstrated the use of microfluidic technology to explore the effects of fluid dynamics, cell phenotype, and cell to cell communication on biofilm formation [34].

In this study, we have developed a microfluidic device from polydimethlsiloxane (PDMS) to examine the biofilm formation in porous media. PDMS is a soft elastomeric polymer which is used for easy and inexpensive fabrication of microfluidic devices. PDMS has obtained significant attraction in the fabrication of devices for the biological research due to its excellent biocompatibility, transparency, and high permeability to different gases such as oxygen. Additionally, mechanical properties of PDMS facilitate the fabrication of fluidic valves and pumps and their integration into microfluidic devices. Full description of the material properties of PDMS can be found elsewhere [35-38]. The following sections describe the microfabrication techniques followed by experimental procedure for growing biofilm and image acquisition in the microfluidic device.

2.2 Design of a 2D porous media mimics

We used three different designs in this study (Figure 2.1). In the first and second design, the main microchannel is 1 cm long, 625 μm wide and 50 μm deep and contains microposts 50 μm in

diameter that are arranged in staggered and uniform porous patterns. The distance between the microposts in each row and column is 25 µm in both patterns. This choice of post diameter and spacing was dictated by considerations such as imaging, fabrication and effect on hydrodynamics. In the third design, we used a combination of microposts with different sizes and different distances between them. In this design, the main microchannel is 1 cm long, 500 µm wide, and 50 µm deep. The dimensions of the porous structures could be found in Table 4.1. The main microchannel connects one outlet and one inlet reservoir (Figure 2.1b). We used a tree like structure at the inlet and outlet of the main channel; similar to what is performed by Cottin *et al.* [39] (Figure 2.1b, *blowout*), to ensure that the pressure head is equal everywhere in the device.

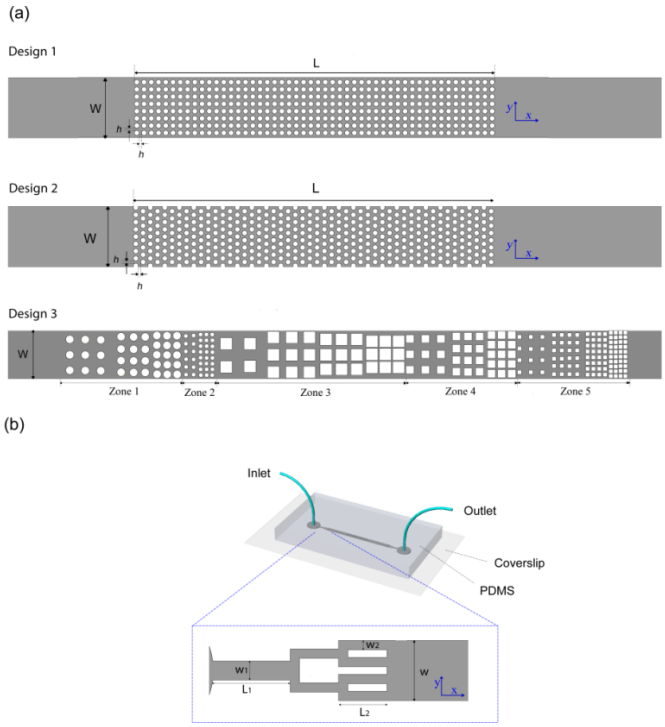

Figure 2.1 a) Design 1: the main microchannel with uniform porous pattern. Design 2: the main microchannel with staggered porous pattern. Design 3: the main microchannel with the combination of different post sizes and distances between the posts. b) A schematic of the microfluidic device used in this study (*blowout:* tree like structure at the inlet of the device)

	Zone 1	Zone 2	Zone 3	Zone 4	Zone 5
D (diameter of posts, µm)	80	40	NA	NA	NA
S (lentgh, µm)	NA	NA	120	80	40
h (pitch, µm)	80, 40, 20	40, 20	120, 60, 40, 20	160, 80, 40	80,40, 20, 10
W (width of the main channel)	500	500	500	500	500

Table 4.1 Important dimensions used in design 3 of microfluidic porous media.

2.3 Microfabrication Techniques

Microfluidic devices in this study were fabricated from PDMS using soft lithography method [40]. Since the final microfluidic channels were fabricated by casting PDMS against a master mold, a silicon master mold was constructed first using standard photolithography process followed by inductively coupled plasma - deep reactive ion etching (ICP-DRIE). Figure 2.2a and 2.2b illustrate the important steps of the photolithography and ICP-DRIE processes, respectively. We used AZ4620 as a positive photoresist in the photolithography process. The photolithography started by printing the design pattern, which is drawn by means of the L-Edit software, on a glass substrate with chrome masking. After fabricating the chrome photomask, following key steps were followed to transfer the designed pattern to the photoresist.

- First, a standard 4′ silicon wafer was chemically cleaned in a piranha solution (H_2SO_4 and H_2O in 3:1 ratio) for 20 minutes. The wafer was then rinsed with DI water and dried. To ensure that the surface was totally dehydrated, the wafer was heated for 15 minutes at 200 ºC on a hotplate.
- A 12.5 µL thick photoresist was spun on the silicon wafer. To achieve the desired thickness, coating was performed in

two steps: a) a spread step for 10 sec at 500 rpm b) a spin step for 25 seconds at 2000 rpm.

- Next, the wafer was soft baked on a hot plate to ensure that the solvent was evaporated. Soft baking was performed in two steps: in step 1, the wafer was floating on a cushion of nitrogen flow at 100ºC for 90 seconds and in step 2, it was kept on vacuum at 100ºC for 60 seconds.
- After soft baking the wafer, a dehydration step was performed by placing the wafer in a dark box for 24 hours.
- After the dehydration period, the wafer was exposed to UV light to transfer the designed porous pattern from the photomask to the photoresist. We used the exposure energy of 730 mJ. The exposure time was calculated by dividing the exposure energy by the exposure factor of the lithography tool.
- Finally, the wafer was immersed in a solution of diluted AZ400K developer for 240 seconds. This step, which is called development step, was intended to remove the exposed parts of the photo resist. At the end, the wafer was rinsed with isopropyl alcohol (IPA) and dried with a gentle stream of nitrogen.

As stated earlier, after the photolithography process, we used plasma induced - deep reactive ion etching (ICP-DRIE) to etch the porous pattern on silicon. The patterned photoresist was resistant to dry-etching and functioned as a masking layer during the process. The masking layer prevented the portions of the silicon wafer that were covered with the photo resist from etching. An etch rate of 0.336 µm/cycle was selected in this step. The etch depth was

chosen to be 50 µm which corresponds to the final depth of the device. After the dry-etching process, the remaining photoresist was removed by acetone and the wafer was cleaned. The prepared master mold was then used in PDMS micromolding process. Figure 2.2c shows the necessary steps for fabrication of a microfluidic device from PDMS. Following steps are necessary to make the final PDMS microchips:

- *Master mold preparation:* The first step in the PDMS casting was the silanization of the silicon master mold. A vial containing a few drops of trichloro(methyl)silane (TCMS) was placed in a desiccator with the master mold under vacuum condition. The monolayer which was formed by silazaniztion agent prevented the silicon master from sticking to the silicon wafer.
- *PDMS preparation and casting:* PDMS was prepared by mixing the Sylgard 184 silicone base and curing agent in a 10:1 ratio by weight. The PDMS was then degassed and poured on the silicon master mold to make the PDMS stamp. After curing the PDMS for 2 hours, the PDMS stamp was peeled off from the master mold and cut into individual microchips.
- *Drilling holes and bonding:* After preparing the PDMS stamps, two holes for inlet and outlet were drilled. The PDMS stamp was then bounded to a cover slip by exposing the PDMS stamp and cover slip to oxygen plasma for 30 seconds. The device is further annealed at 70ºC for 10 min to achieve a good sealing.

To examine the accuracy of the micro fabrication process, SEM images of the PDMS stamp were captured, which can be seen in Figure 2.3. From the Figure 2.3, it is evident that all the walls are vertical with an extremely smooth surface.

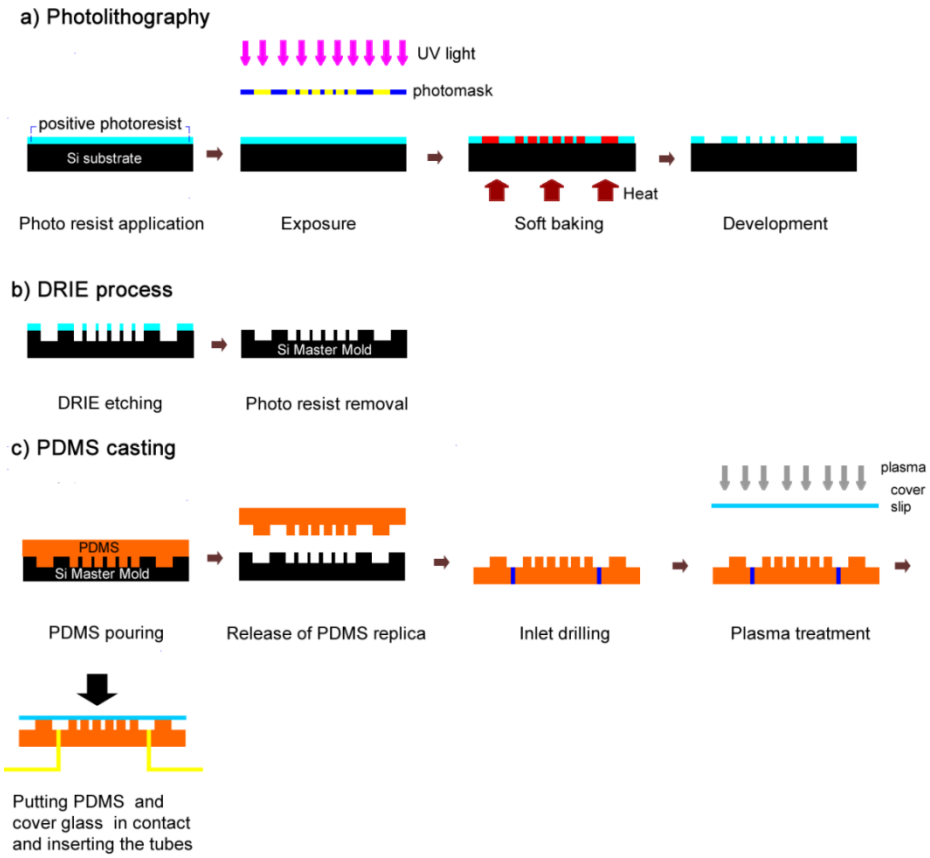

Figure 2.2 A schematic of the required steps for fabrication of a microfluidic device from PDMS. (a) Required steps for the Photolithography process. (b) Required steps for DRIE processes. (c) Required steps for fabricating the master mold which will be used to fabricate the final PDMS microchips

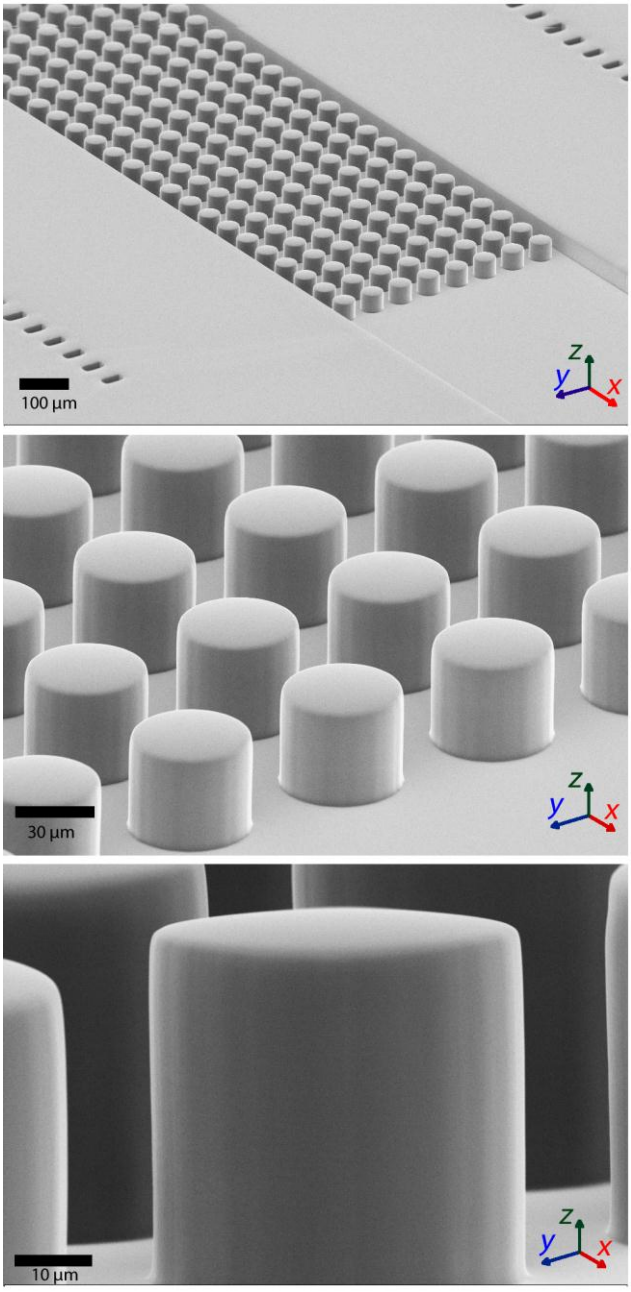

Figure 2.3 SEM images of the micropostsat at different magnifications.

2.4 Experimental setup: biofilm growth and image acquisition

We used wild type and ΔgacS mutant of *pseudomonas fluorescens* bacterial strains in this study. We obtained the bacterial strains from Professor Howard Ceri's Lab at Biological Sciences Department of the University of Calgary. *Pseudomonas fluorescens* is a Gram negative aerobic biofilm forming bacterium that is found in soil and plays an important role in the promotion of

plant health [41]. The wrinkly spreader (WS) is a colony morphology variant of the mutant that is missing gacS sensor kinase. This variant produces more biofilm mass which is probably caused by overproduction of exopolysaccharide cellulose. Both these stains express green fluorescent protein (GFP) constitutively. The inoculum was prepared by growing bacterial colonies in LB broth medium at 30°C and 220 rpm overnight (Appendix A contains a summary of the microbiological techniques that are used in this study). The optical density of bacterial culture at 600 nm (OD_{600}) was measured with a spectrophotometer in the exponential growth phase. To ensure that the bacterial concentration is constant in each experiment, OD_{600} is set to 0.1 prior to injection by performing serial dilutions using sterilized LB broth. Figure 2.4 shows the schematic of the setup used in this study. We used Tygon tubing to connect the inlet to a syringe pump and the outlet to a waste reservoir containing disinfectant solution. The device was disinfected by exposure to UV light and loaded on the stage of an inverted confocal laser scanning microscope (Carl Zeiss, Inc., NY, USA). A 70% ethanol solution was injected before the introduction of bacterial solution to ensure that the microfluidic chamber is sterile. Bacterial solution was infused continuously using a syringe pump (Harvard Apparatus, MA, USA). The temperature of the microfluidic device was set to 30°C during the experiment using an on-stage microscope incubator (Live Cell instruments, South Korea). The spatial-temporal changes of the biofilm were observed using 40X, 20X, and 10X objectives. Images at different positions in the chip were collected using microscope image software.

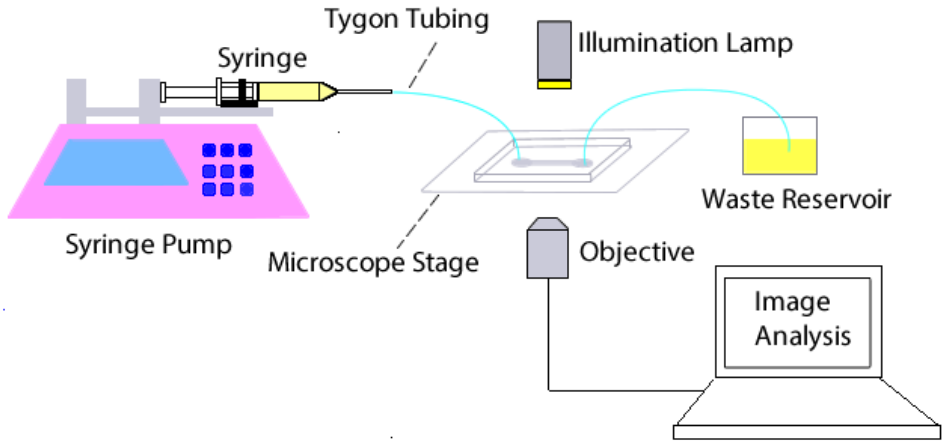

Figure 2.4 A schematic of the experimental setup used for growing and monitoring of biofilms in microfluidic porous media.

2.5 Summary

In this chapter, we first presented the design and microfabrication techniques for the fabrication of a porous microfluidic device. Our microfluidic device, which is made with PDMS, contains an array of uniform and staggered microposts. The microfabrication techniques that we used offer a great potential for the microfabrication of the PDMS microfluidic devices with the minimum fabrication errors. We also explained the experimental procedure for the biofilm formation and image acquisition. The results of the biofilm formation will be discussed in the next chapter.

3 Streamer formation in porous media[1]

3.1 Introduction

In chapter one, we learned that that there is a complex interaction between biofilm formation and hydrodynamic conditions in porous matter. Given the relevance of biofilm growth in porous media in many industrial and environmental operations, considerable amount of research has aimed to understand this complex interaction. Earlier research works have mainly investigated the influence of biofilm formation in porous media on the bulk fluid properties such as porosity, permeability, flow rate, and pressure drop [19, 42-45]. In these works, quantitative measurements were performed to demonstrate that biofilm accumulation in porous media results in the significant decrease in the permeability and porosity as well as increase in the friction factor and dispersivity of the media. Different experimental setups with sizes ranging from a few millimetres to several meters have been used to study the effect of biofilm progression on porous media hydrodynamics. A comprehensive list of different studies on the effect of biomass development on hydrodynamic properties of porous media can be found in reference [19].

While it is well established that bacterial accumulation influences the hydrodynamic properties in porous media, local hydrodynamic conditions have also been reported to influence the biofilm accumulation. The effect of fluidic conditions on the morphology of biofilms has been studied by different researchers.

[1] Some parts of this chapter has been published in *Lab on a Chip* journal, 2012, Vol. 12, Pages 5133-5137

In these studies, it is shown that the change in flow regime affects the thickness, homogeneity, continuity, roughness, surface coverage, and other morphological features of biofilms in porous media [46-50]. It is also demonstrated that the development of different biofilm patterns is highly correlated to change in the porosity, permeability, and dispersion of the flow, which implies a complex and dynamic relationship between the biofilm morphology and hydrodynamic conditions in porous media [49, 51].

Of the various studies dedicated to understanding the effect of hydrodynamics on the aggregation and growth of biofilms, few studies have observed the existence of filamentous structures in porous media. Filamentous biofilm structures have already been reported to form in natural flow environments such as rivers even in the extreme harsh environments such as arctic cold saline springs, hydrothermal hot springs and metal-rich acidic waters [52-54]. Since these filamentous structures exhibit a streamlined shape in natural environments; they are usually referred to as streamers. Streamers are tethered to a surface on one or both the ends, while the rest of the structure is floating in the fluid. Stoodley et al. observed the formation of streamers between the pore spaces of an artificial porous media fabricated by packing glass beads in a flow cell chamber [22]. They further suggested that these filamentous structures have a remarkable effect in changing the friction factor and pressure drop of the flow within the porous media. Filamentous structures also have been observed to form in 2D porous micromodels and their substantial contribution to the fluid

flow diversion in porous media has been demonstrated [23, 24, 55, 56].

While previous studies have revealed some aspects of the biofilm streamers, this interesting phenomenon is still poorly understood. In particular, to the best of our knowledge, no comprehensive data on role of hydrodynamics on the formation, morphology and distribution of biofilm streamers in porous media is available in the literature. This suggests that further research is needed to investigate the process of streamer formation and its inter-relationship with concomitant transport processes.

Using a microfluidic porous media mimics in this study, we observed the formation of streamers between the microposts in our microfluidic device after flushing the bacterial solution for a few hours. Additionally, we found that streamer formation in our device was strongly correlated to hydrodynamics, and that the fluid flow could be responsible both for the appearance and destruction of such streamers. Finally, we noted that streamers were distributed throughout the height of the device, which is interesting as it differs from the observation of single streamers in the mid-section of curved channels by Rusconi *et al.* [33].

3.2 Temporal evolution of streamers

We first examined the biofilm formation in our microfluidic device by injecting the wild type strain at the constant flow rate of 0.8 µL/hr into the microchannel. Not surprisingly, bacterial attachment and biofilm formation occurred on the bottom (z = 0), top (z = 50 µm), and lateral surfaces of the micro channel as well as on the surface of the PDMS micro posts. After 24 hours of experiment, no sign of biofilm structures on any other place except the surfaces

was observed. Next, we increased the flow rate to 8 μL/hr. As in the previous case, bacteria form biofilm on different surfaces in the micro channel at the beginning of the experiment. However, interestingly, following the infusion of solution for a few hours, we observed the appearance of filamentous structures consisting of few bacteria in the inter pillar region between the top and bottom surface of the micro channel, at various *z*-locations (Figure 3.1). Streamers are viscoelastic filamentous biofilm structures that develop in fast flows and here they are tethered to the posts, but the rest of the structure is surrounded only by fluid. These streamers are formed by strands of EPS, with bacteria embedded in the EPS matrix. The initial streamers trailed nearly parallel to the direction of the main flow (aligned with *x*-axis), so we refer to them as parallel streamers. Figure 3.1 and Figure 3.2 depict the temporal evolution of a streamer located between two pillars using confocal laser scanning microscopy (CLSM). At the beginning, streamers are as thick as the width of a single bacterium ($\approx$0.8 um). With time, streamers grew thicker in diameter and turned into a mature thick streamer. The growth of streamers was assisted through the incorporation of planktonic microbes as well as bacterial growth. As the time progressed, bacterial streamers increased in number as well. In addition, formation of streamers which are not aligned with either the *x* or *y* axes were observed. We call these streamers transverse streamers. Streamer formation in our device was extensive, and after sufficient time, these streamers formed a 'web' that could connect different pillars. The ΔgacS mutant also formed streamers under these conditions, but no significant difference between the morphology of streamers of the wild-type and the

mutant was observed. Temporal evolution of streamers formed by the ΔgacS is depicted in Figure 3.3.

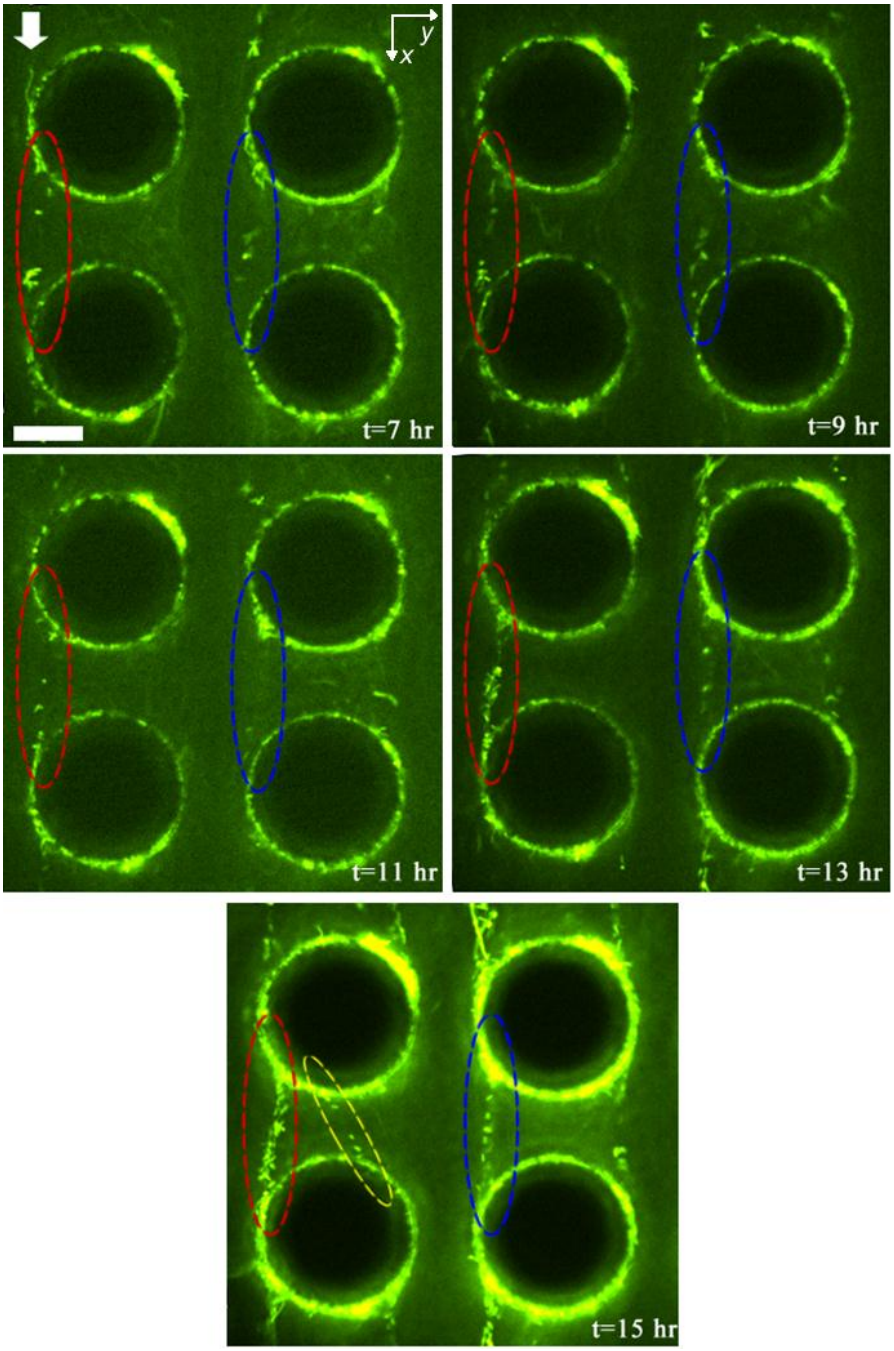

Figure 3.1 Time evolution of streamers at the flow rate of 8 µL/hr. Red, blue and yellow ellipses show the position of streamer structures (scale bar is equivalent to 20 µm and the white arrow shows the direction of the flow).

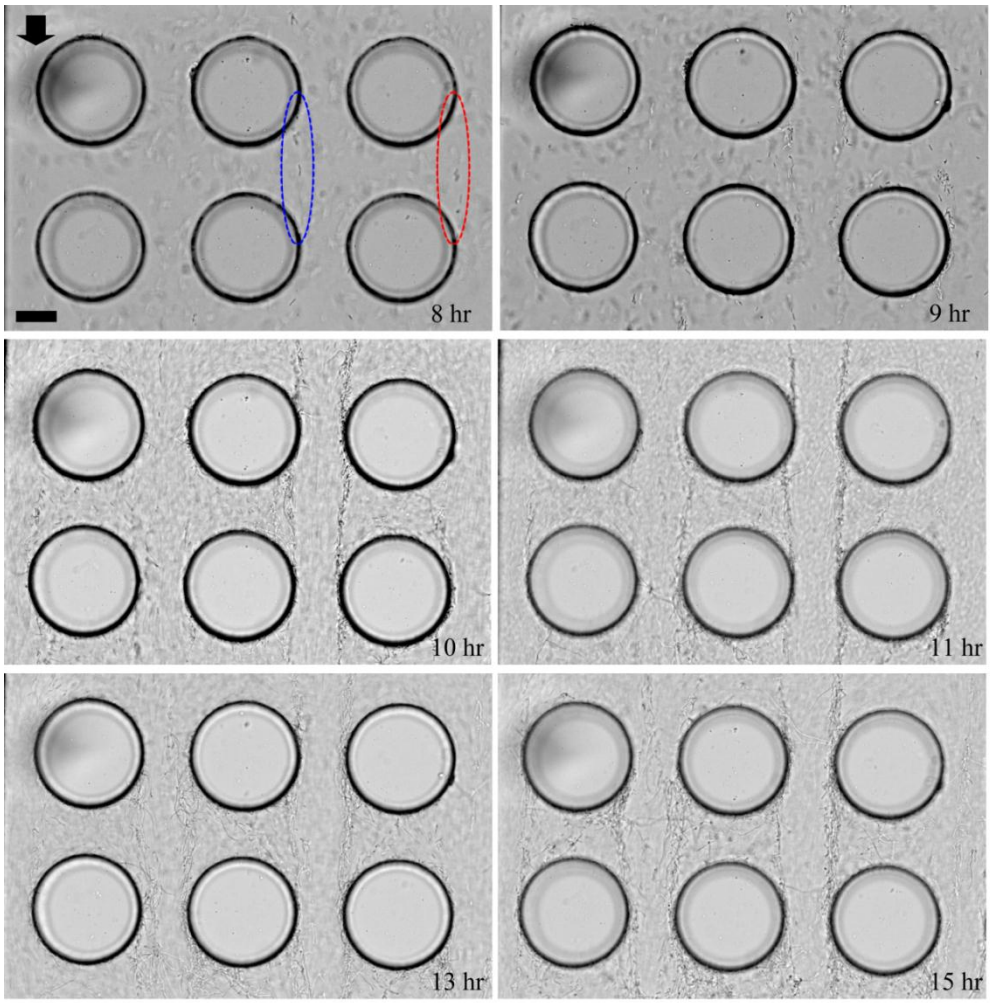

Figure 3.2 Bright field images of evolution of streamers at the flow rate of 8 µL/hr. Blue and red ellipses show streamer structures at the initial stages (scale bar is equivalent to 20 µm and the black arrow shows the direction of the flow).

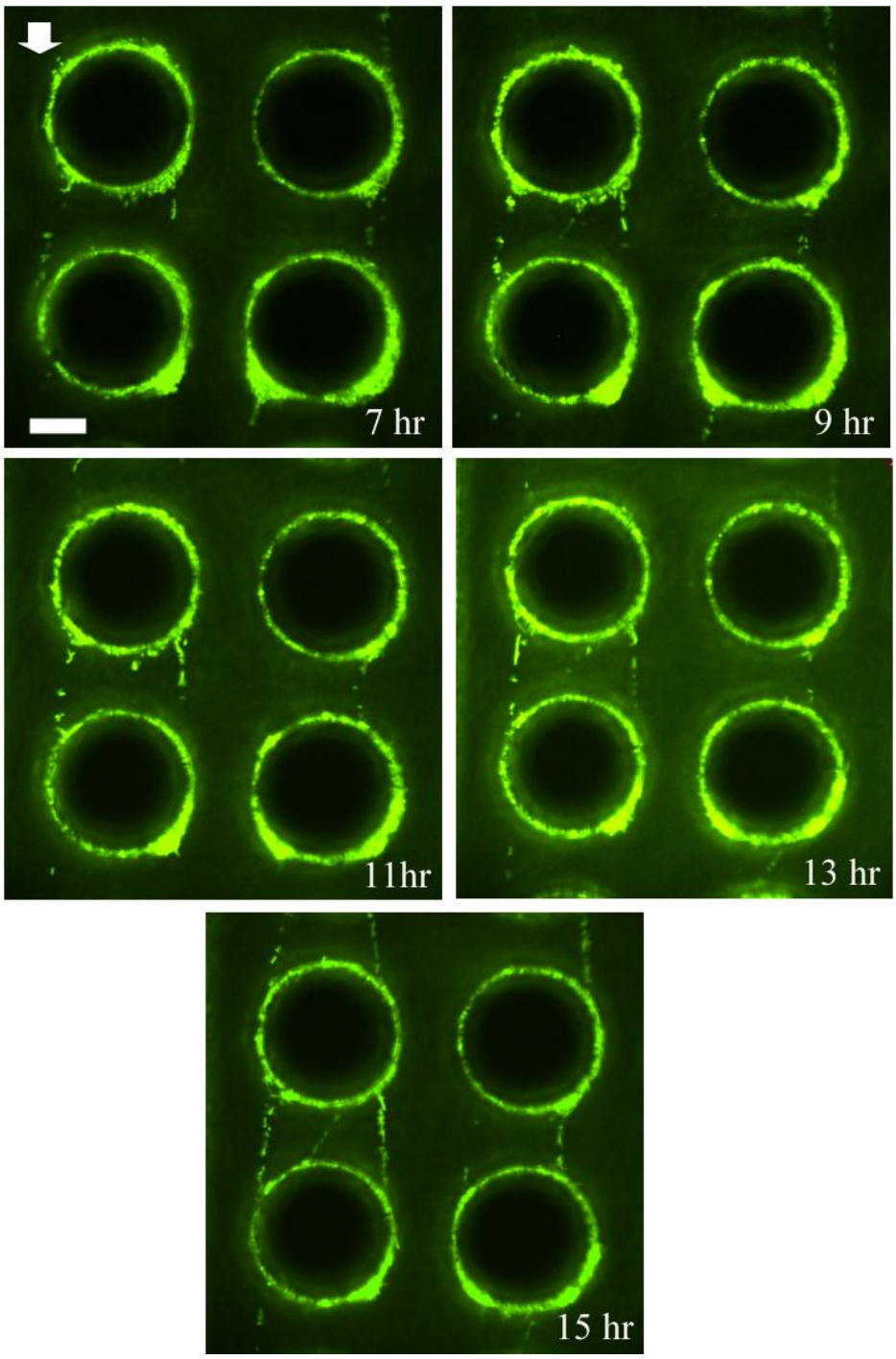

Figure 3.3 Time evolution of streamers formed by mutant strain at the flow rate of 8 µL/hr (scale bar is equivalent to 20 µm and the white arrow shows the direction of the flow).

3.3 Effect of flow rate on streamer formation

To further investigate the streamer formation in porous media, experiments were performed at the flow rates of 12, 20, and 80 µL/hr and streamer evolution was monitored at the same period as the previous experiments. Our experimental data demonstrated that there is a strong connection between the fluid flow and production of streamers. Streamer formation occurred at the flow rates of 12 and 20 µL/hr, however no permanent streamer formation was observed at the flow rate of 80 µL/hr. Figure 3.4 and Figure 3.5 show the formation of streamers for the flow rates of 12 and 20 µL/hr, respectively. As in the case of flow rate of 8 µL/hr, streamer development began with the formation of very thin filaments within the porous media. These streamers then grew with time until they occupied a large portion of the interpillar region. Formation of both parallel and transverse streamers was observed for both flow rates. In addition, at the flow rates of 12 and 20 µL/hr, we observed the migration of the streamers from the upstream section as is marked by red ellipses in Figure 3.4 and Figure 3.5. The migration of these streamers is probably resulted from the higher shear stress and drag force in higher flow rates that result in larger expansion of the viscoelastic streamers.

Although it was seen that streamers form at the flow rates of 8, 12, and 20 µL/hr, but there was a perceptible change in the dynamics of the process. Figure 3.6a compares the morphology of streamers after 9 hours of experiment for different flow rates at the same region throughout the porous media. The first effect of flow rate on the streamer formation is the change in the onset time of streamer formation. In other words, the higher the flow rate, the

earlier the streamers appeared in microchannel. Figure 3.6b shows the number of streamers for 6 pillars at a fixed position. Only transverse and parallel streamers are taken into account in counting the streamers. From the figure, it could be easily deduced that the average initial lag time, which corresponds to appearance of the first streamer throughout the fixed region, is higher at larger flow rates. Secondly, streamers grew much faster in higher flow rates resulting in higher number of streamers at each time point. The number of streamers can be compared from the confocal image sidebars shown in Figure 3.6a after 9 hours of experiment. The growth in the number of streamers can also be quantitatively compared from the plot shown in Figure 3.6b. This plot clearly shows that the numbers of streamers are higher at each time point at higher flow rates. The words A and B represent the last time points that counting the individual streamers was possible for flow rates of 20 µL/hr and 12 µL/hr. The high number of thick streamers makes it difficult to recognize individual streamers after these time points. Thirdly, increase in the flow rate not only caused the formation of higher number of streamers at each time point, but also resulted in the formation of thicker streamer structures. From Figure 3.6a, it is clear that while the streamers are still very thin in the flow rate of 8 µL/hr, they have already occupied a large portion of the inter-pillar region at the flow rate of 20 µL/hr. Although these trends demonstrate that the flow rate affects the dynamics of streamer formation, the relation between the flow rate and streamer formation seems to be very complex. The flow rate determines the attachment and detachment of the microbes as well as mass transport of the nutrients and bacteria. It is recently proposed that

the flow rate even influence the biological phenomena such as secretion of EPS [57]. Hence, the link between flow rate and streamer formation is far beyond a straightforward simple relationship and further investigations need to be done in this respect. At the flow rate of 80 µL/hr, we observed transient formation of streamers, but permanent structures did not form. These transient structures were washed away with time, depicting that fluid stresses can also play a destabilizing role in streamer formation. These observations indicate that streamer formation is a result of competing forces, and hence favourable hydrodynamic conditions need to prevail for streamer formation.

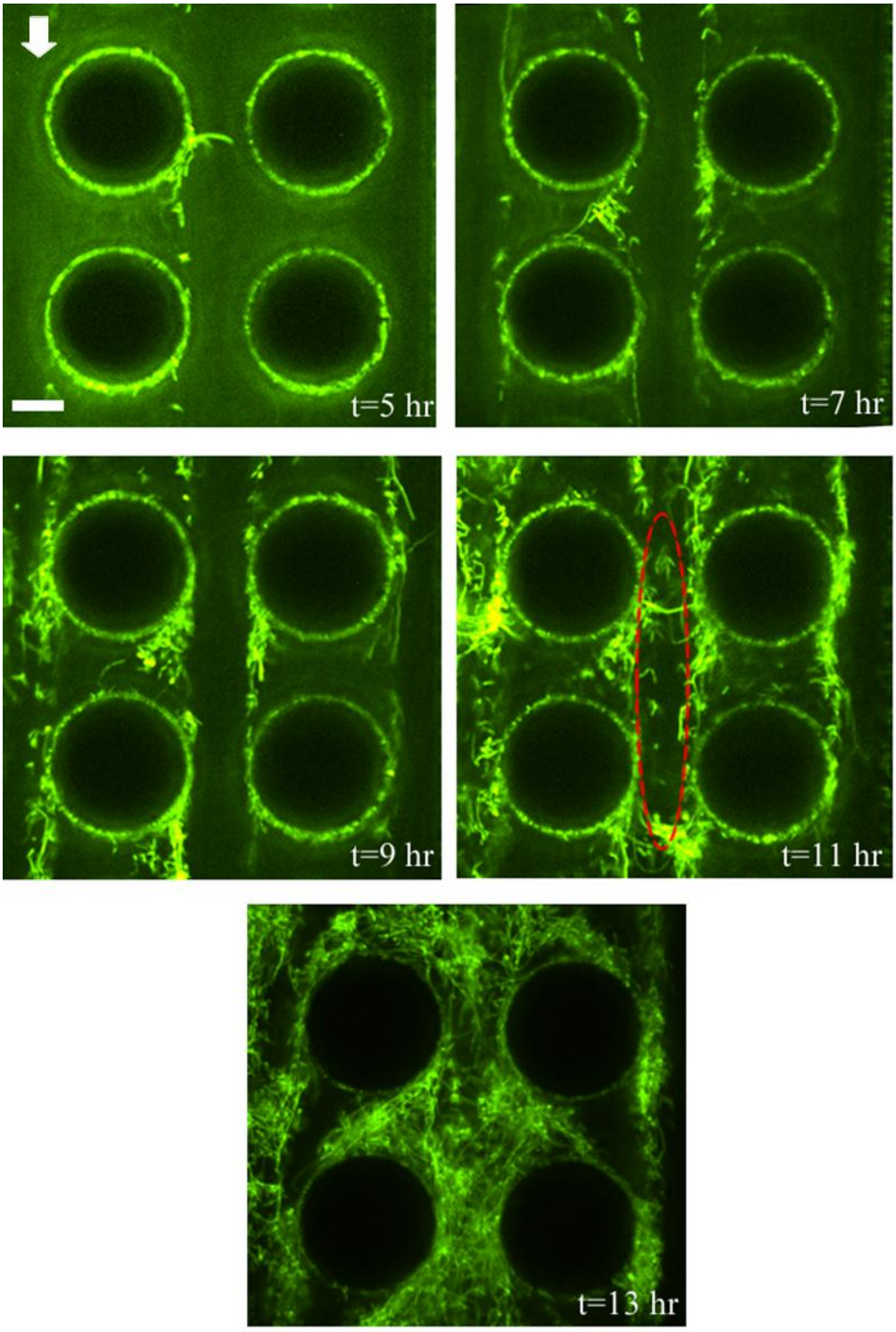

Figure 3.4 Time evolution of streamers at the flow rate of 12 µL/hr (scale bar is equivalent to 20 µm and the white arrow shows the direction of the flow).

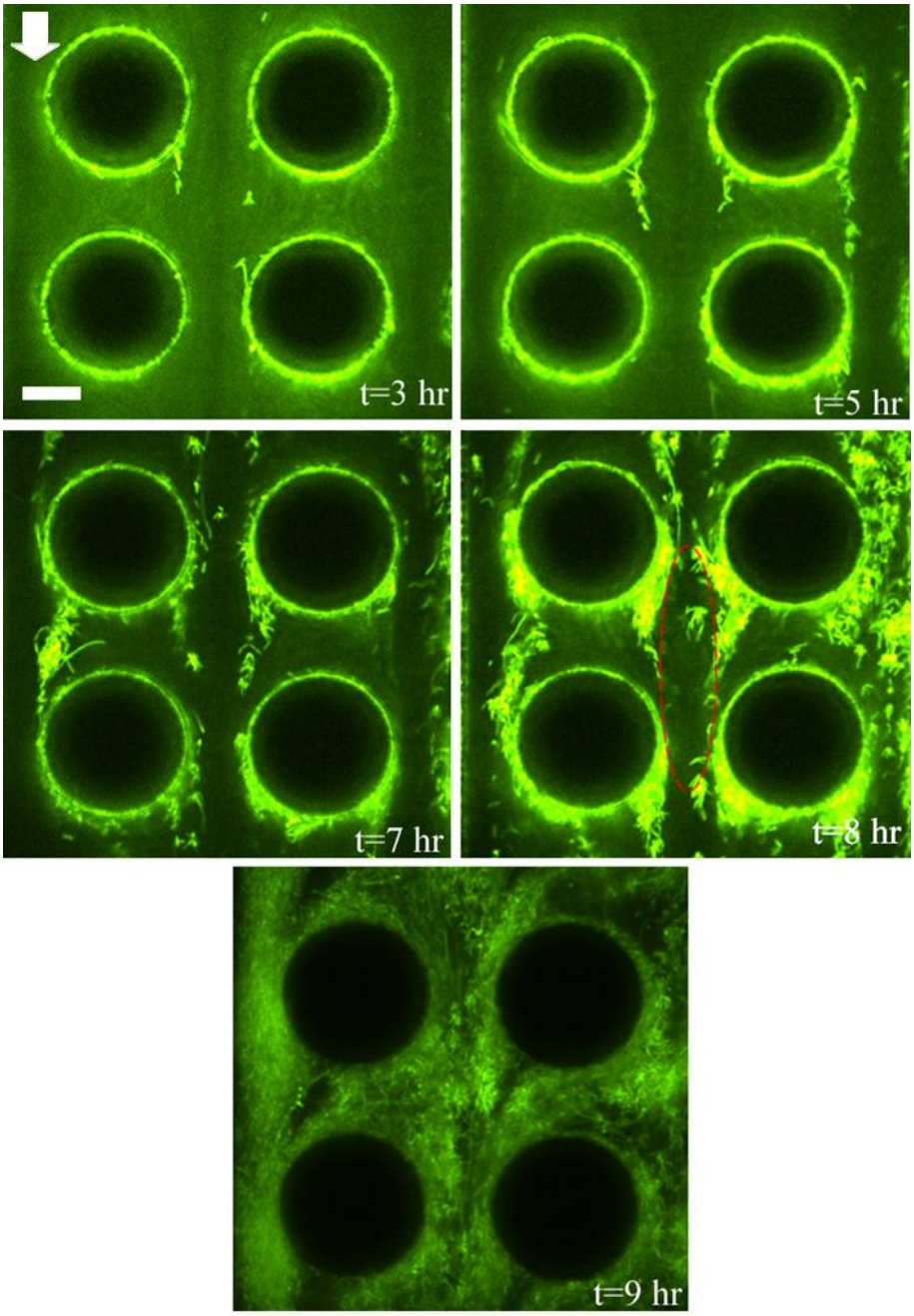

Figure 3.5 Time evolution of streamers at the flow rate of 20 μL/hr (scale bar is equivalent to 20 μm and the white arrow shows the direction of the flow).

(a)

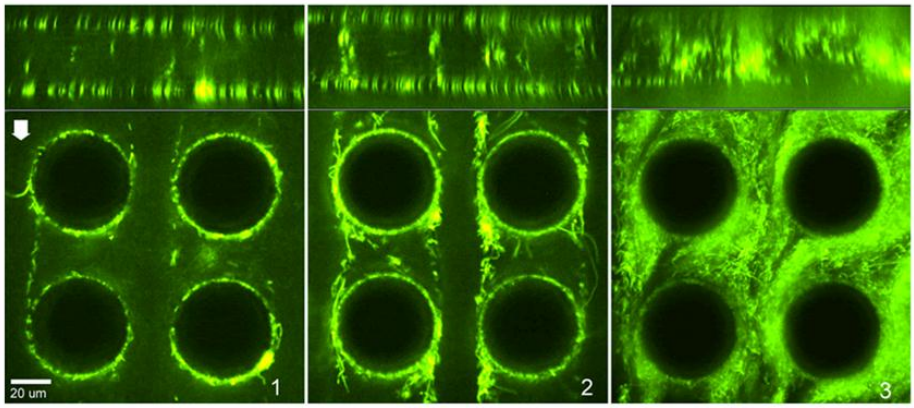

(b)

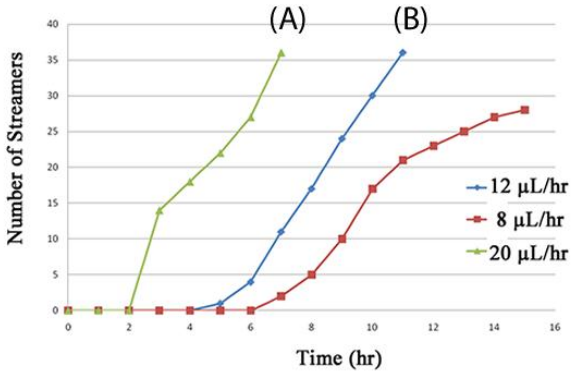

Figure 3.6 a) Confocal images of the evolution of streamers after 9 hour of experiment (side bars show the distribution of streamers along the channel). b) Number of streamers versus time for different flow rates.

3.4 Spatial organization of streamers

Confocal microscopy allowed us to determine the *z*-locations of the streamers. Figure 3.7- Figure 3.9 illustrate a series of confocal images captured at five different focal planes at the flow rate of 8, 12, and 20 uL/hr. The z-stack images at the bottom (*z*=0) and the top (z=50 μm) surfaces indicate the formation of a relatively uniform biofilm on these surfaces. By contrast, the confocal images captured at *z*=1/4 H, *z*=3/4 H, and *z*=1/2H (H=height of the pillars) demonstrate the formation of filamentous structures between the pillars at these focal planes. The pictures also show higher number of streamers at the middle plane (*z*=1/2 H) compared to other planes (*z*=1/4 H, *z*=3/4 H). To further elucidate the quantitative distribution of streamers along the channel depth, an area consisting of 24 pillars was selected as shown in Fig. 3.10. To facilitate the analysis, the height of middle point of each streamer was regarded as the height of that streamer. The number of streamers at the selected area was counted for each 5 um height intervals after 15 hours of experiment and was plotted in a histogram shown in Figure 3.10. In the same way, the number of streamer versus their *z*-locations was plotted for the flow rates of 12 and 20 μL/hr after 9 and 5 hours, respectively. Both parallel and transverse streamers were taken into account in counting the streamers. The histogram for the flow rate of 8 μL/hr shows no streamer formation at the proximity of the surface (at a distance less than 10 μm). Although, there is a very small symmetry in the number of streamers on both sides of the micro-channel, the number of streamers increases as we go to the mid-section of the device. Similarly, although the distribution becomes less

symmetric in the flow rates of 12 µL/hr and 20 µL/hr, the number of streamers is still higher in the central region of device similar to the flow rate of 8 µL/hr.

Appearance of a large number of separate streamers distributed all along the channel height in our porous geometry stands in contrast to the formation of a single streamer in the centre of a microfluidic device with curved channels as reported by Stone's group [33]. The researchers suggested a link between the formation of streamers and secondary flows that occur in the proximity of the corners. We will investigate the effect of hydrodynamics on streamer formation using numerical modelling of the problem in Chapter 4.

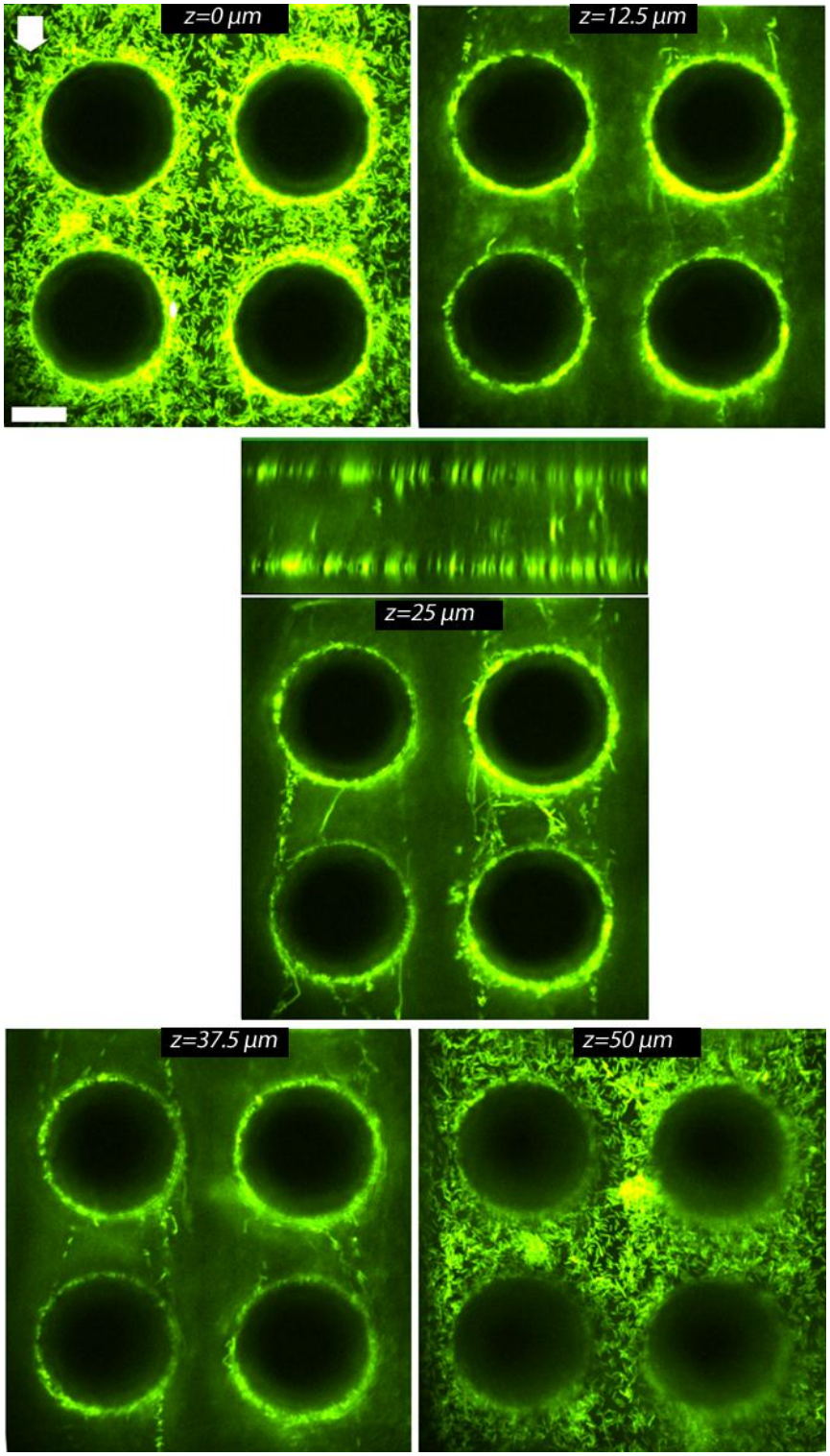

Figure 3.7 Confocal images of streamers at five different z-locations of the channel, i.e. z= 0, z=25, z=50, z=75, z=100 µm, after 15 hours of experiment at the flow rate of 8 µL/hr (white arrow shows the direction of the flow, scale bar is equivalent to 20 µm).

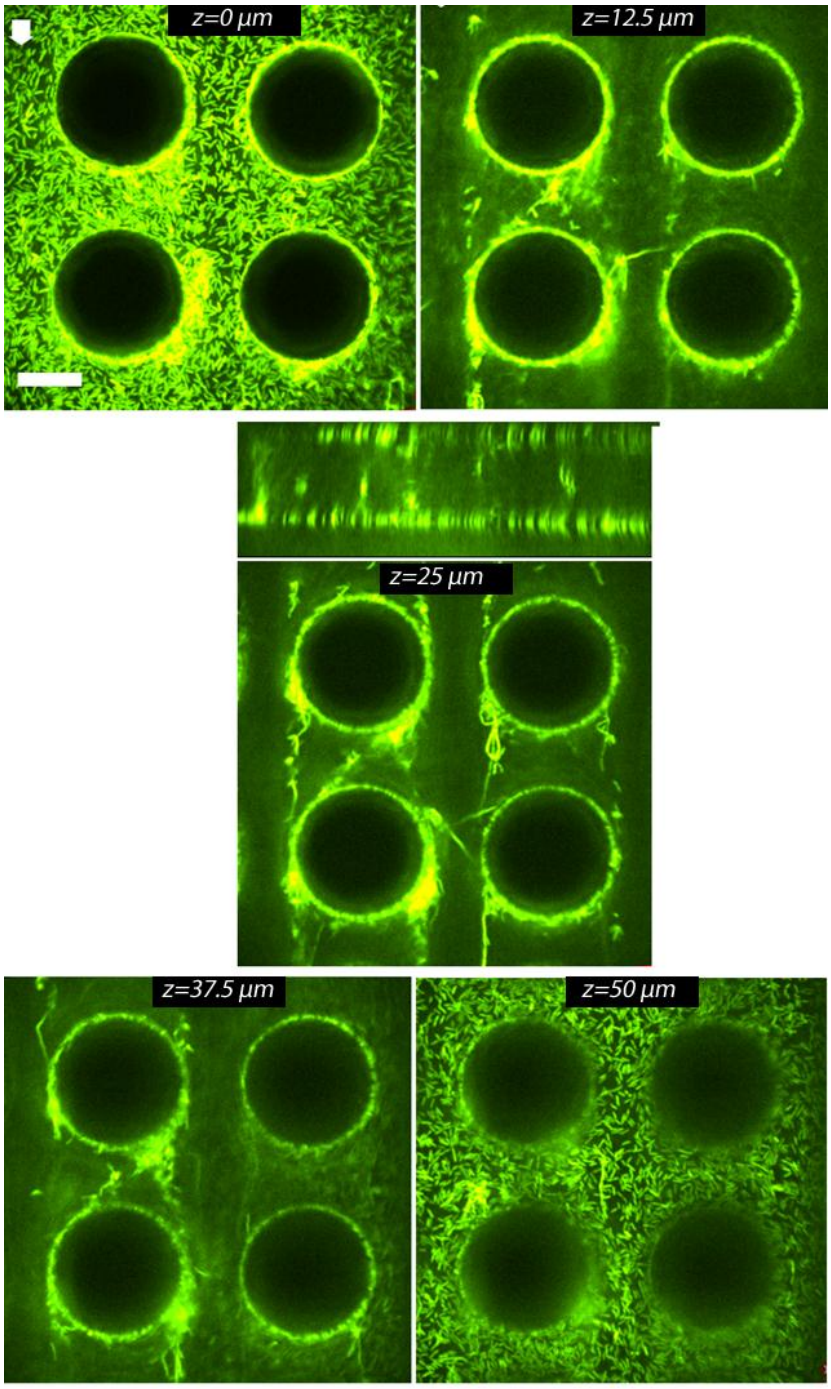

Figure 3.8 Confocal images of streamers at five different z-locations of the channel, i.e. *z*= 0, *z*=25, *z*=50, *z*=75, *z*=100 µm after 9 hours of experiment at the flow rate of 12 µL/hr (white arrow shows the direction of the flow, scale bar is equivalent to 20 µm).

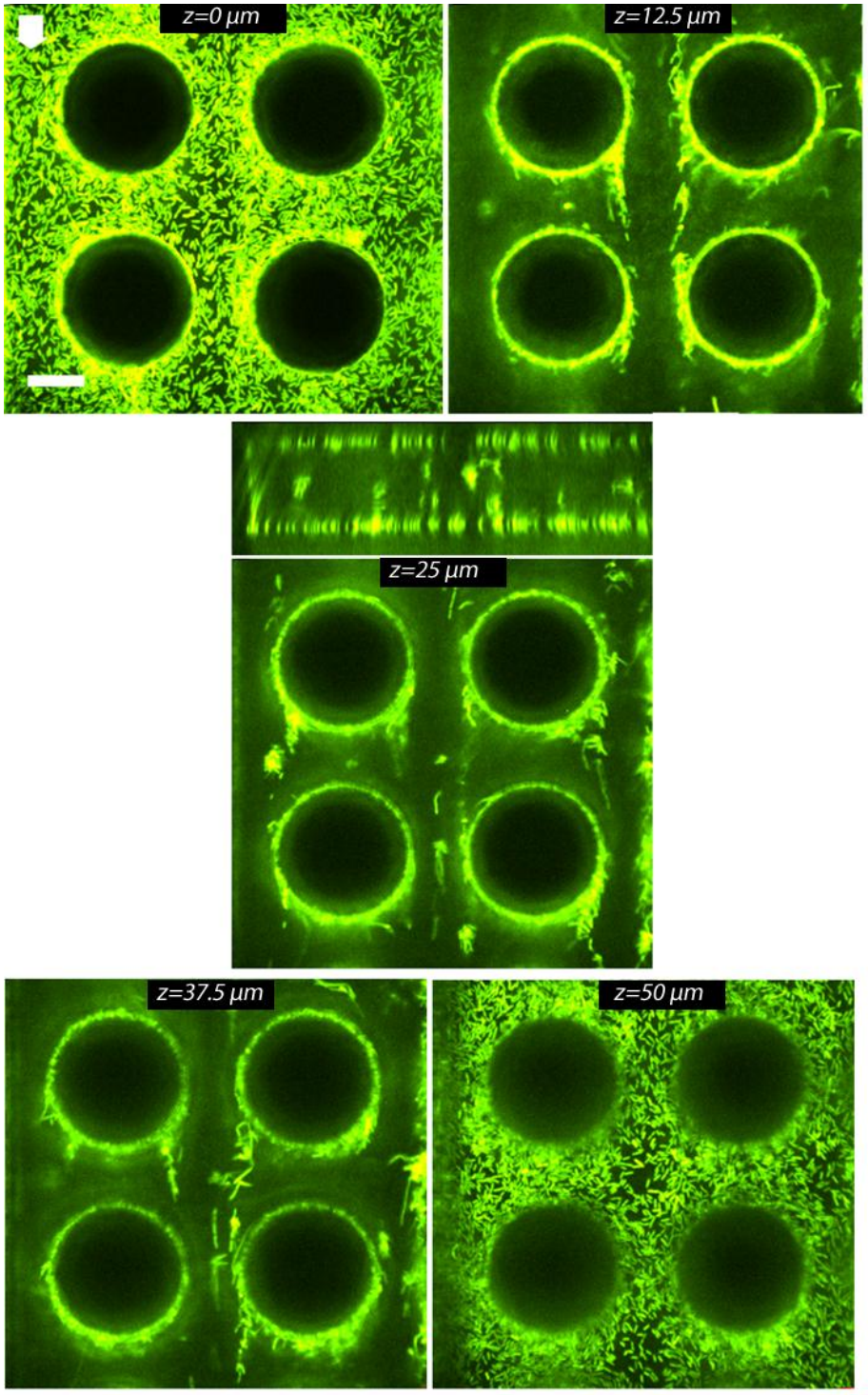

Figure 3.9 Confocal images of streamers at five different z-locations of the channel, i.e. *z*= 0, *z*=25, *z*=50, *z*=75, *z*=100 µm after 5 hours of experiment at the flow rate of 20 µL/hr (white arrow shows the direction of the flow, scale bar is equivalent to 20 µm).

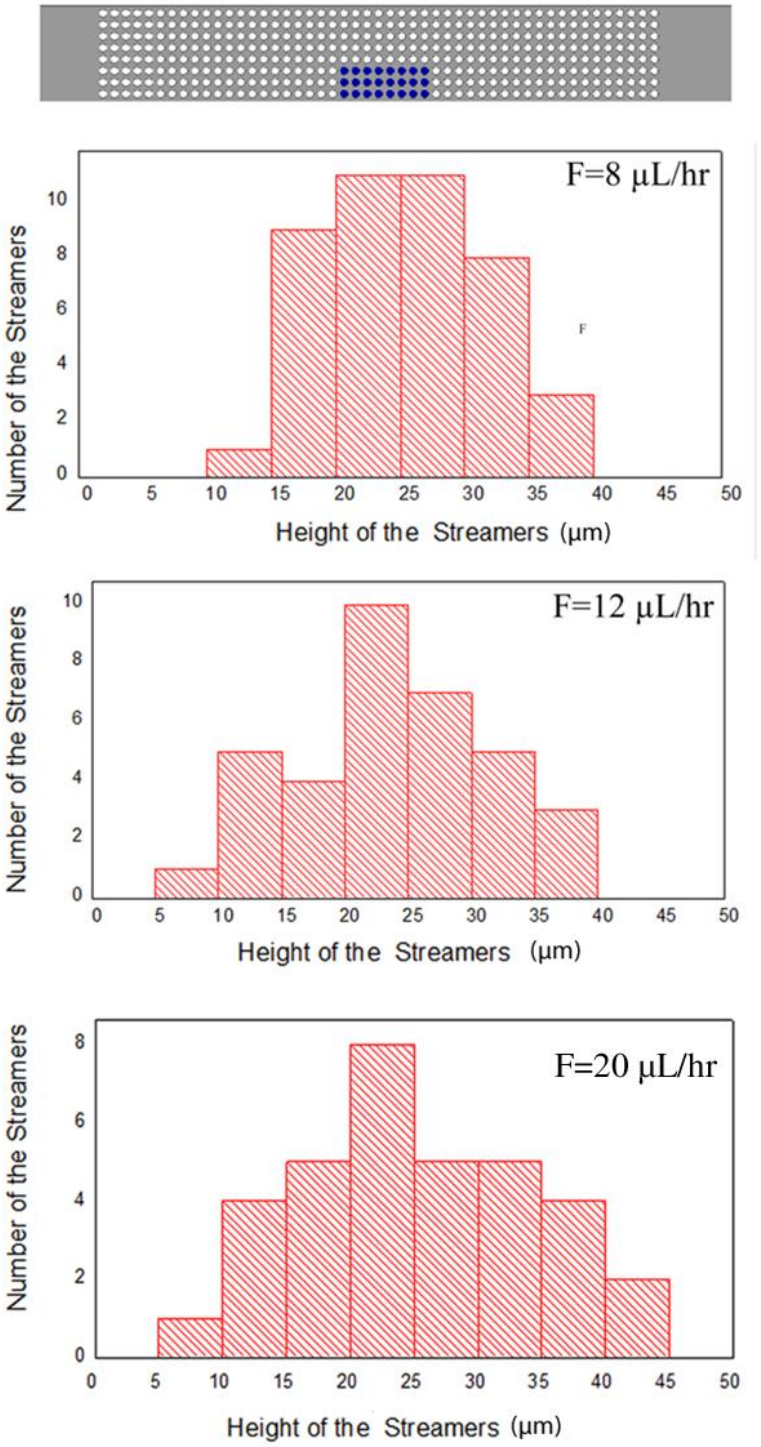

Figure 3.10 Distribution of the streamers along the height of the channel for different flow rates of 8, 12, 20 µL/hr after 15, 9, 5 hours of experiment (area of the porous zone selected for calculating the number of streamers is shown on top of the histogram).

3.5 Preliminary studies on the streamer formation in different porous patterns

We have also observed the formation of streamers for the porous media with staggered pattern of microposts. Figure 3.11 shows the temporal evolution of streamers for staggered pattern porous media. Streamer formation in the staggered pattern initiated by appearance of a few bacteria in the inter pillar region similar to what was already observed for the uniform porous pattern. Streamers grew with time and created a repeated web like pattern throughout the porous media. Figure 3.12 shows the extensive formation of streamers within the staggered pattern porous media. These observations demonstrate that while the basic features of the streamers is the same for different geometries, the final structure and pattern varies from one geometry to another.

We also tested the biofilm formation in the porous patterns with different porosities. Figure 3.13 shows the morphology of streamers for different porosities. It is clear that streamers develop faster in the porous media with lower porosities creating denser structures at the same time points. This could be attributed to the higher fluid velocities between the pillars in the devices with lower porosities, however further research is needed to identify the effect of porosity on the streamer formation in porous media. Finally, we have observed that streamer formation is not limited to the device with circular micropost and streamers even form in the device with square micro posts Figure 3.14 and 3.15).

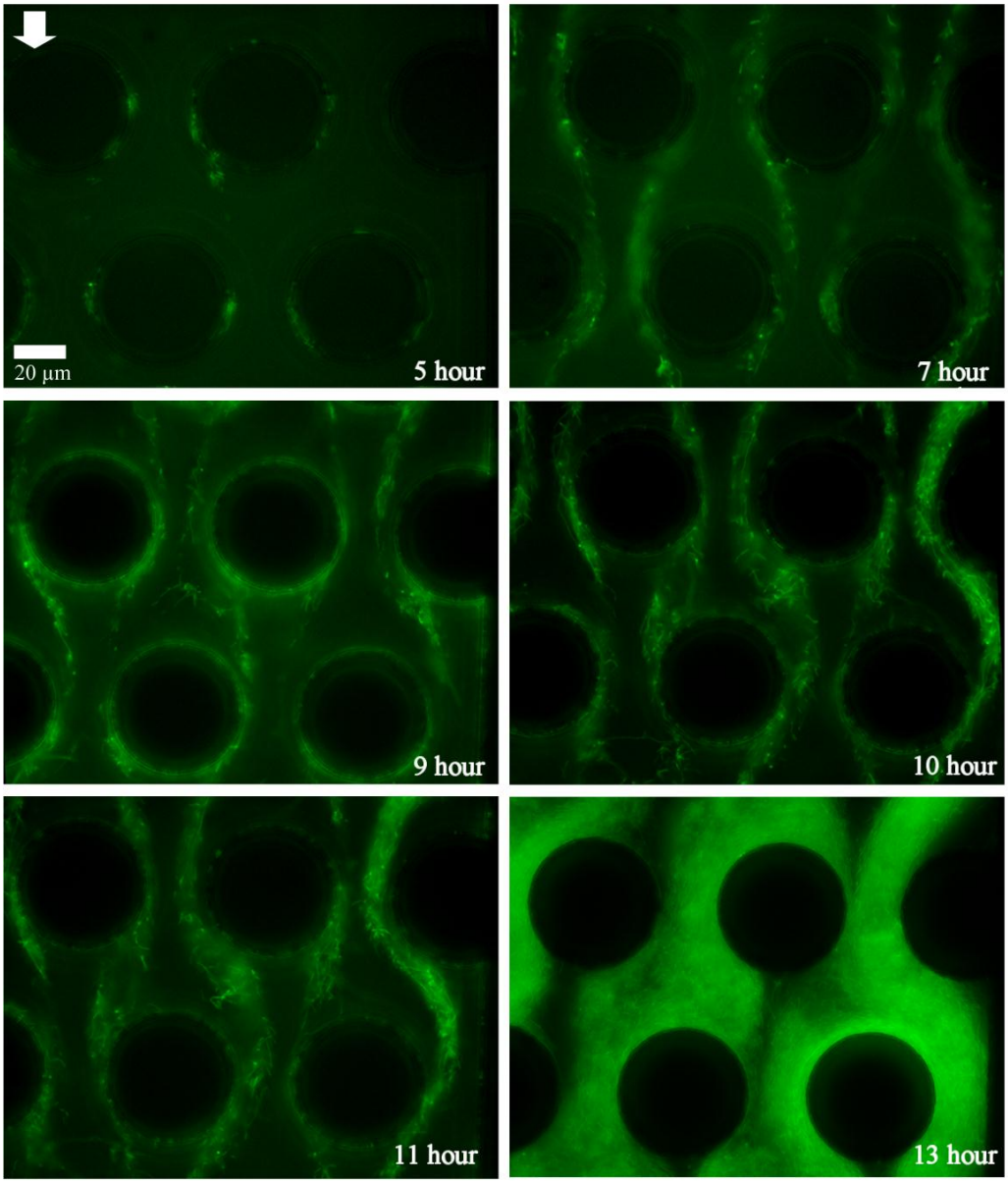

Figure 3.11 Temporal evolution of streamers at the flow rate of 12 µL/hr (scale bar is equivalent to 20 µm, white arrow shows the direction of the flow)

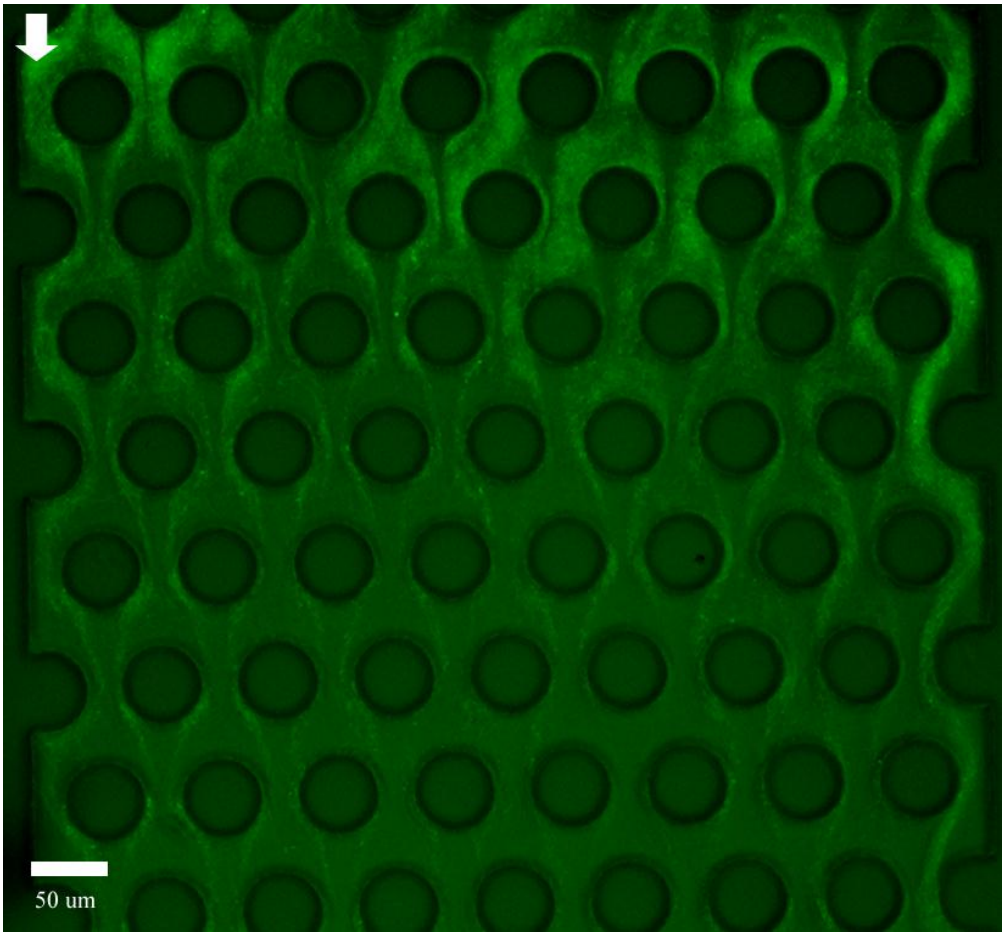

Figure 3.12 Extensive formation of streamers throughout the microchannel with staggered pattern (white arrow show the direction of the flow)

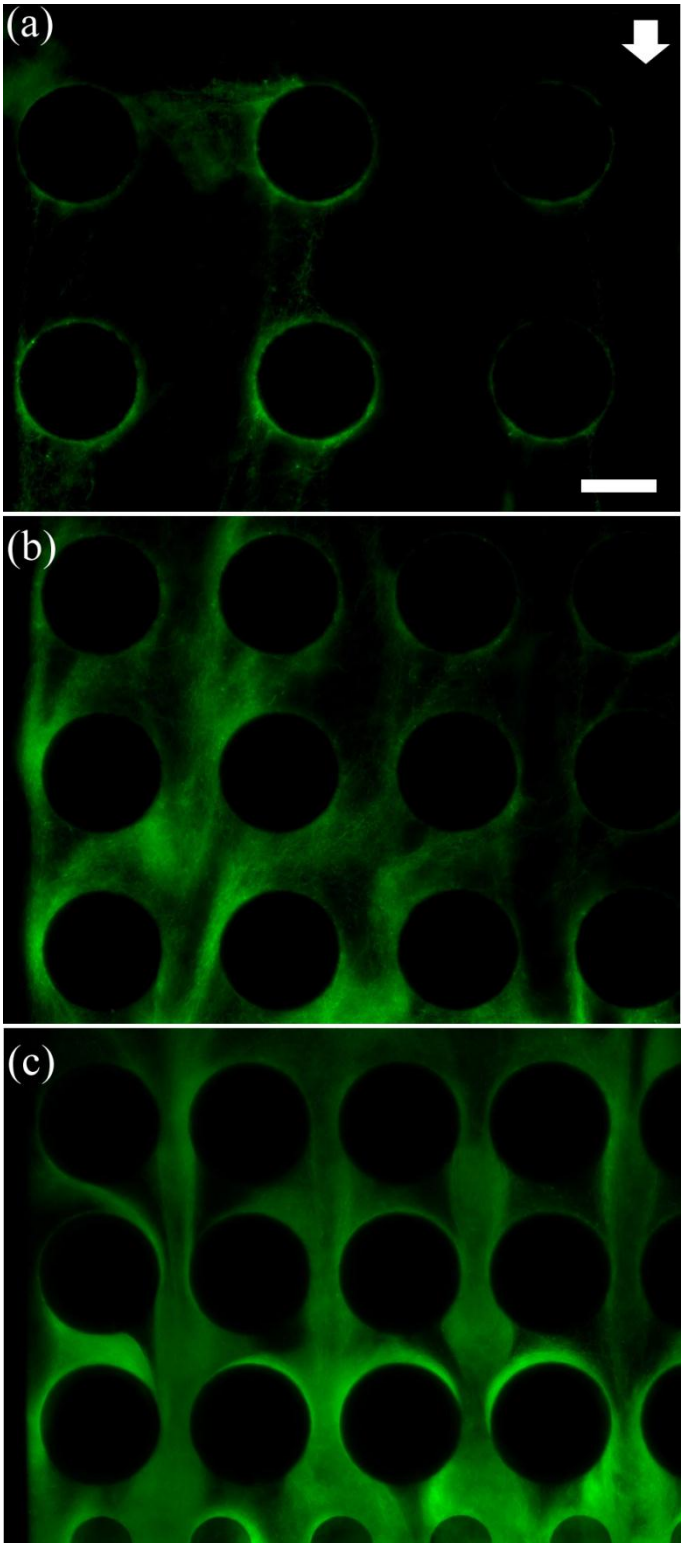

Figure 3.13 Streamer formation in the porous patterns with different porosities after 18 hours of experiment at the flow rate of 8 µL/hr (zone 1 in the design 3, white arrow shows the direction of flow, scale bar is equivalent to 40 µm).

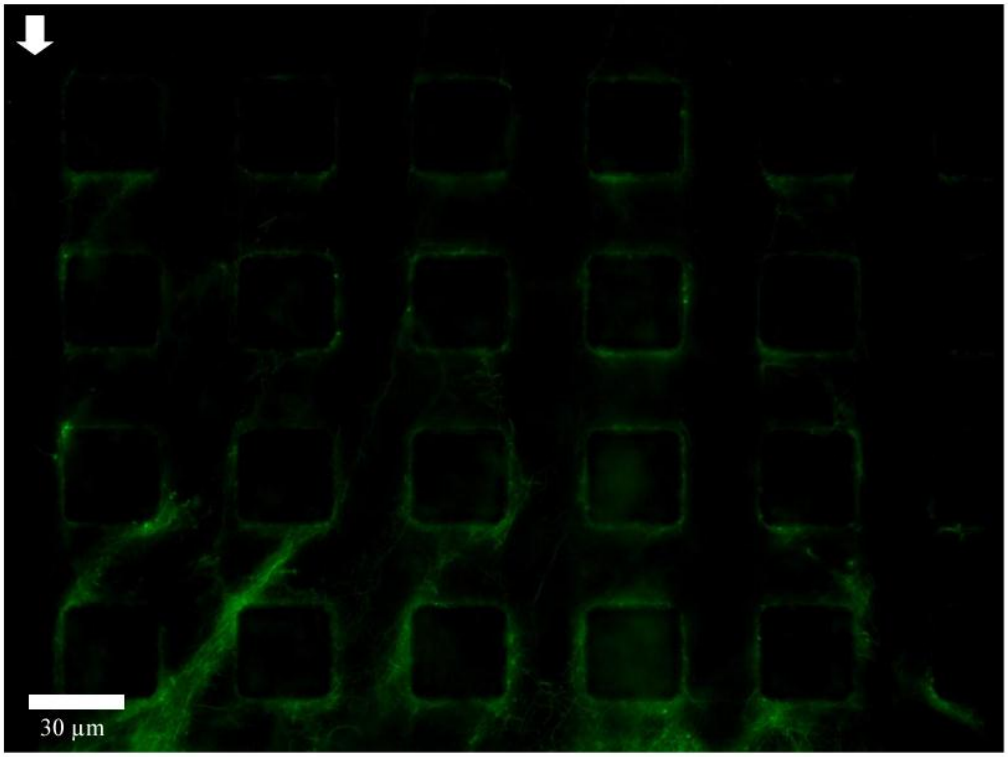

Figure 3.14 Streamer formation in the device with square micro posts (white arrow shows the direction of flow).

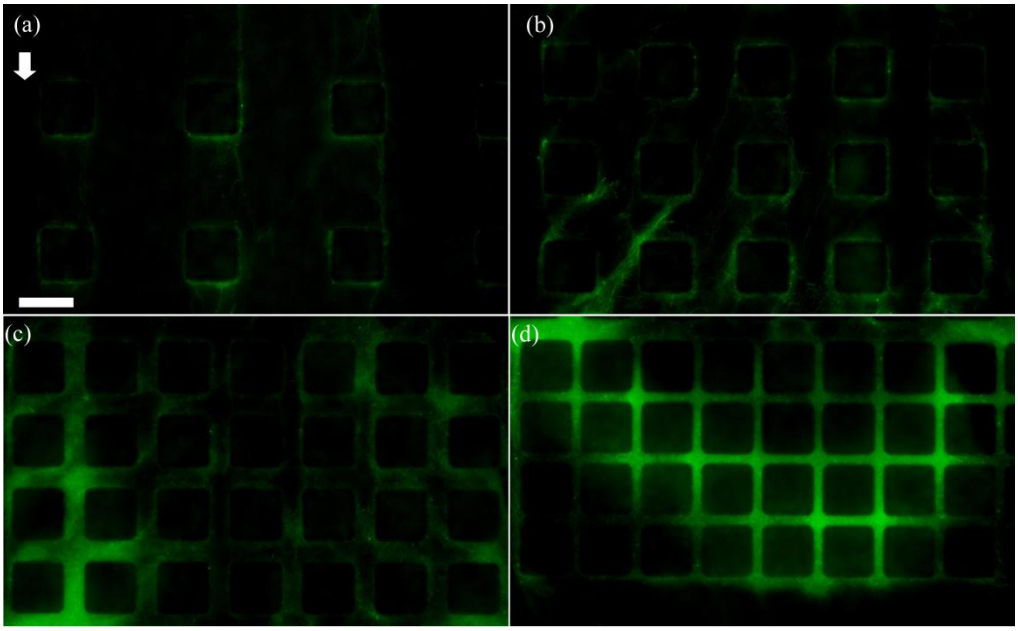

Figure 3.15 Streamer formation in the porous media with uniform square posts at different porosities (zone 5 in design 3, white arrow shows the direction of flow, scale bar is equivalent to 40 µm).

3.6 Summary

In this chapter, we have seen that the biofilm morphology in our microfluidic device, which contains an array of microposts in a microchannel, mainly consists of filamentous structures known as streamers. We have also seen that the streamer formation is not limited to device with uniform pattern of micro posts and filamentous structure formed in other arrangements of micro posts such as staggered pattern as well. We investigated the temporal evolution and spatial organization of these streamers as a function of fluid flow in our device. We found that the formation of streamers only occurred within a certain flow rate range in our device. Moreover, even within this range, streamer formation dynamics and morphology change prominently with the change in flow rate. These observations suggest a strong link between the streamer formation and hydrodynamic conditions. In the next chapter, we will use numerical simulation to model the fluidic condition in our device and will investigate its connection with the formation of streamers.

4 Biofilm development and fluidics

4.1 Introduction

Emergence of the field of microfluidics has generated a new approach for studying fluid dynamics problems in different disciplines. Of particular interest is the application of microfluidics to study the behaviour of microorganisms in different fluidic conditions. Most of microorganisms live in viscous dominated fluidic conditions, where inertial forces are unimportant. The main criterion for determining this flow regime, which is called laminar flow, is the small value of the Reynolds number. The Reynolds number is a dimensionless number which shows the relative importance of inertial and viscous forces and is defined as $\mathrm{Re} = \rho VL/\mu$, where ρ and μ indicate the fluid density and viscosity, respectively, and V and L represent the velocity and length scale of the flow, respectively. In the previous chapter, we reported the formation of biofilm streamers in a porous microfluidic device under laminar flow conditions and studied their spatial and temporal properties. In this chapter, we use numerical simulation to understand the hydrodynamic condition in our device and its link with the formation of biofilm streamers.

4.2 Problem formulation for numerical simulation

In order to understand the inter-relation between streamer formation and hydrodynamics in our device, we performed fluid mechanical simulations with Comsol Multiphysics® (Boston, MA). COMSOL Multiphysics is engineering simulation software, which can numerically solve various multiphysics problems using the finite element methodology.

For our computer aided design (CAD) model, we used the geometrical parameters used in the actual experiments. As our system is microfluidics in nature, the flow in the channel belongs to the laminar flow regime, and even more specifically to the creeping flow regime (*Re*<<1). Under these conditions, the flow typically changes linearly with input conditions. Hence, simulations performed at a certain input condition, e.g. flow rate, can often be used as a representative description of the flow behaviour. Assuming the constant inlet flow velocity of 8 µL/hr in the simulation as the representative flow rate, the Reynolds number of 8×10^{-3} was calculated using the appropriate hydraulic diameter, which further demonstrates the presence of the laminar flow regime throughout the microfluidic device. Since under the laminar flow regime, the formation of secondary flows and eddies are known to occur in certain geometrical features, we attempted to make a three dimensional formulation of the problem in order to evaluate the effect of three-dimensional (3D) flow features on the formation of streamers. Hence, the fluid flow in the microchannel is described by incompressible Navier-Stokes and continuity equations as follows:

$$\rho(\mathbf{u}.\nabla)\mathbf{u} = \nabla.[-p\mathbf{I} + \mu(\nabla\mathbf{u} + (\nabla\mathbf{u})^T] + \mathbf{F} \qquad \text{Eqn. 4.1 (Navier-Stokes)}$$

$$\nabla.(\rho\mathbf{u}) = 0 \qquad \text{Eqn. 4.2 (Continuity)}$$

Boundary conditions that are used to solve the above equations are:

$$\mathbf{u}\big|_{\text{walls except inlet and outlet}} = \mathbf{0} \qquad \text{Eqn. 4.3 (No Slip)}$$

$$\mathbf{u}\big|_{\text{inlet}} = -U_0\mathbf{n} \quad (U_0 = 4 \times 10^{-5}\ \text{m/s}) \qquad \text{Eqn. 4.4 (Velocity)}$$

$p\big|_{\text{outlet}} = p_0$ (P_0 =101.325 KPa) Eqn. 4.5 (Pressure)

Once the equations and boundary conditions were set, the domain was discretized using the software predefined physics controlled mesh. The flow was solved in the steady state mode and mesh refinements were performed to obtain the convergence of the solution (Figure 4.1 shows a 2D and 3D schematic of the refined meshed geometry)

4.3 Simulation Results

The important features of the simulation results are illustrated in Figures 4.2 to 4.5. Figure 4.2 shows the velocity magnitude in a cross section of the device located at ¼ of the height of channel from the bottom surface of the microchannel. In order to understand the three dimensional flow features, we also plotted the z- component of the velocity in a plane located at ¼ of the height of channel from the bottom surface of the microchannel in Figure 4.2b. Even though the flow at the inlet boundary has no z-component, the presence of a nonzero *z*-component of the velocity around the pillars demonstrates the existence of secondary flows superimposed on the primary flow in the vicinity of the pillars. These primary and secondary flows are further illustrated at different points in a *yz* plane at the upstream and downstream parts of a pillar in Figure 4.3. This figure shows the secondary flow consists of two eddies that have opposite directions and converge at centre of the device. As this figure shows, the directions of the secondary flow changes after the side points of a pillar (compare Figure 4.3a,b with Figure 4.3c,d). In other words, the orthogonal components of velocities are divergent at the upstream section of

the pillars while they become convergent at the downstream part of the pillars. This three dimensional feature of the flow around a cylinder, which is believed to be caused by the curvature of the boundary, has been examined in the previous studies [58, 59]. The secondary flow is very small and constitutes less than 10 % of the total velocity. In order to acquire a better understanding of the variation of velocity profiles in the device, the magnitude of primary and secondary velocities and associated streamlines are plotted in a *xy* plane for uniform pattern in Figure 4.4. The streamline plot demonstrates the presence of a pair of vortices between the pillars. This feature has been experimentally investigated by Taneda *et al*. and only exist when the pillars are closer than a certain limit [60]. The same flow features are also plotted in Figure 4.5 for the staggered pattern. As in the case of uniform pattern, it is evident that the small secondary flow in the z direction is present in the staggered pattern which has similar properties to the secondary flow in the uniform pattern. However; the streamline plot shows that no vortex exists between the pillars (in the *xy* plane) in the staggered pattern porous media. Other hydrodynamic parameters such as shear stress and pressure are also depicted in Figure 4.6.

4.4 Link between the streamer formation and hydrodynamics

In the previous chapter, we observed the formation of biofilm streamers along the height of the channel between two pillars. Stone's group has already observed the formation of a single biofilm streamer in the centre of the device with curved channels and attributed the formation of the biofilm streamers to the secondary flow around the corners [61]. They suggested that the

accrual of biomass by secondary flows to the middle of the device is probably the underlying mechanism for the formation of biofilm streamers. On the other hand, we observed the appearance of large number of streamers across the channel which stands in contrast to the observation of a single streamer in the device with curved channels. Thus while secondary flow occurs in our device structure too, the observation of streamers at locations other the device mid-plane indicates that they do not play a dominant role. Similarly the effect of vortices between the pillars seems to be unimportant since the streamer formation occurs in the staggered pattern, where no vortex is present in the interpillar region. Even though streamer formation is a function of the imposed flow rate, the correlation with other hydrodynamic properties is also not straightforward. For example, parallel streamers form near regions of higher velocities and correspondingly higher shear rates (please refer to Figure 4.6), but transverse streamers form near regions of lower velocities. Thus, the correlation between hydrodynamics and streamer formation is not straightforward and requires further research. Streamer formation seems to be a very intricate and complex process and there remain several unexplained facets of its development.

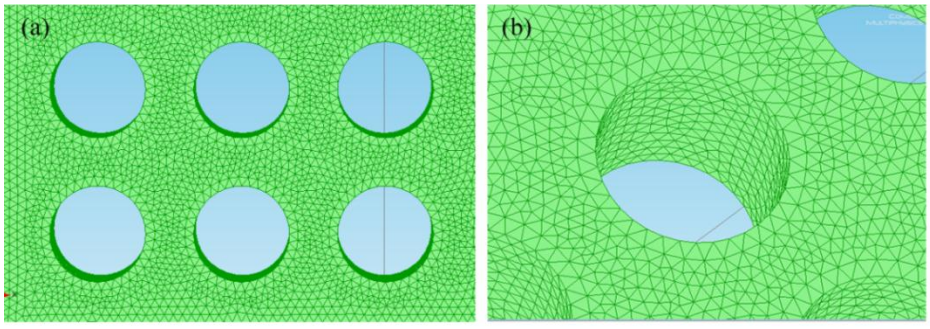

Figure 4.1 a) A 2D and b) a 3D schematic of the meshed geometry.

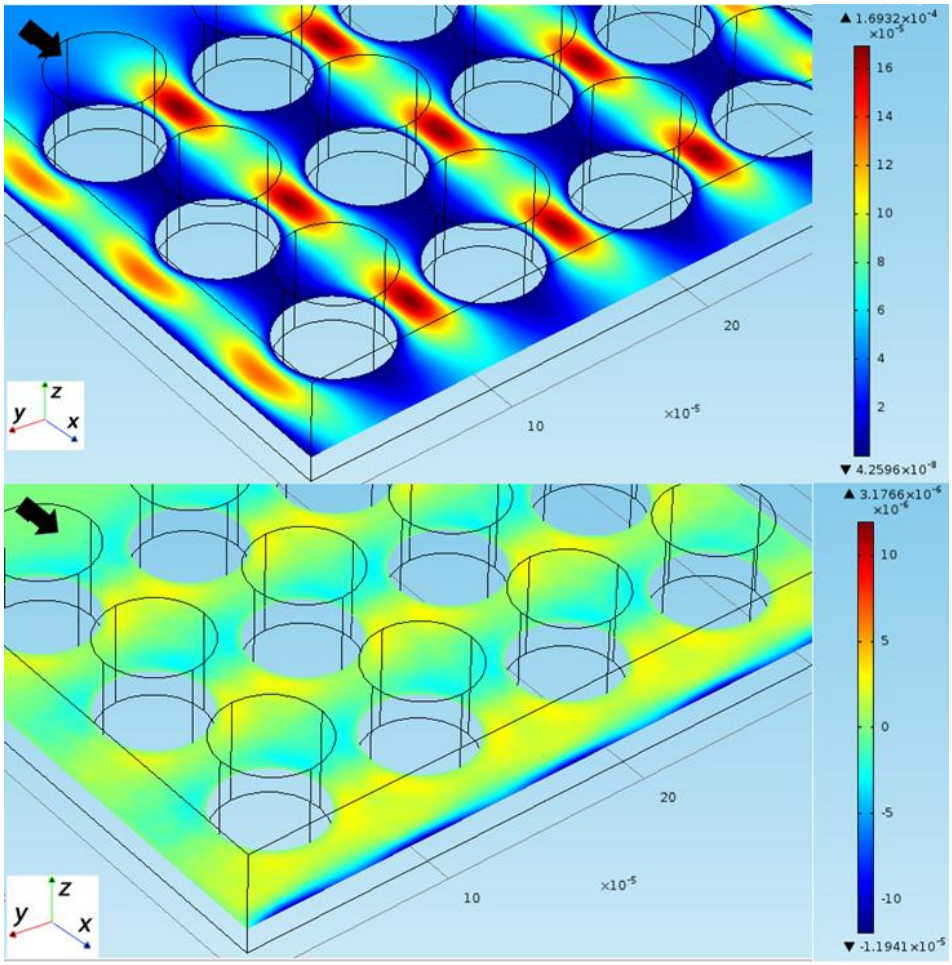

Figure 4.2 (a) Numerical results of the modulus of the velocity field in a plane located at ¼ of the channel height from the bottom surface b) *z* component of the velocity in the same plane**.**

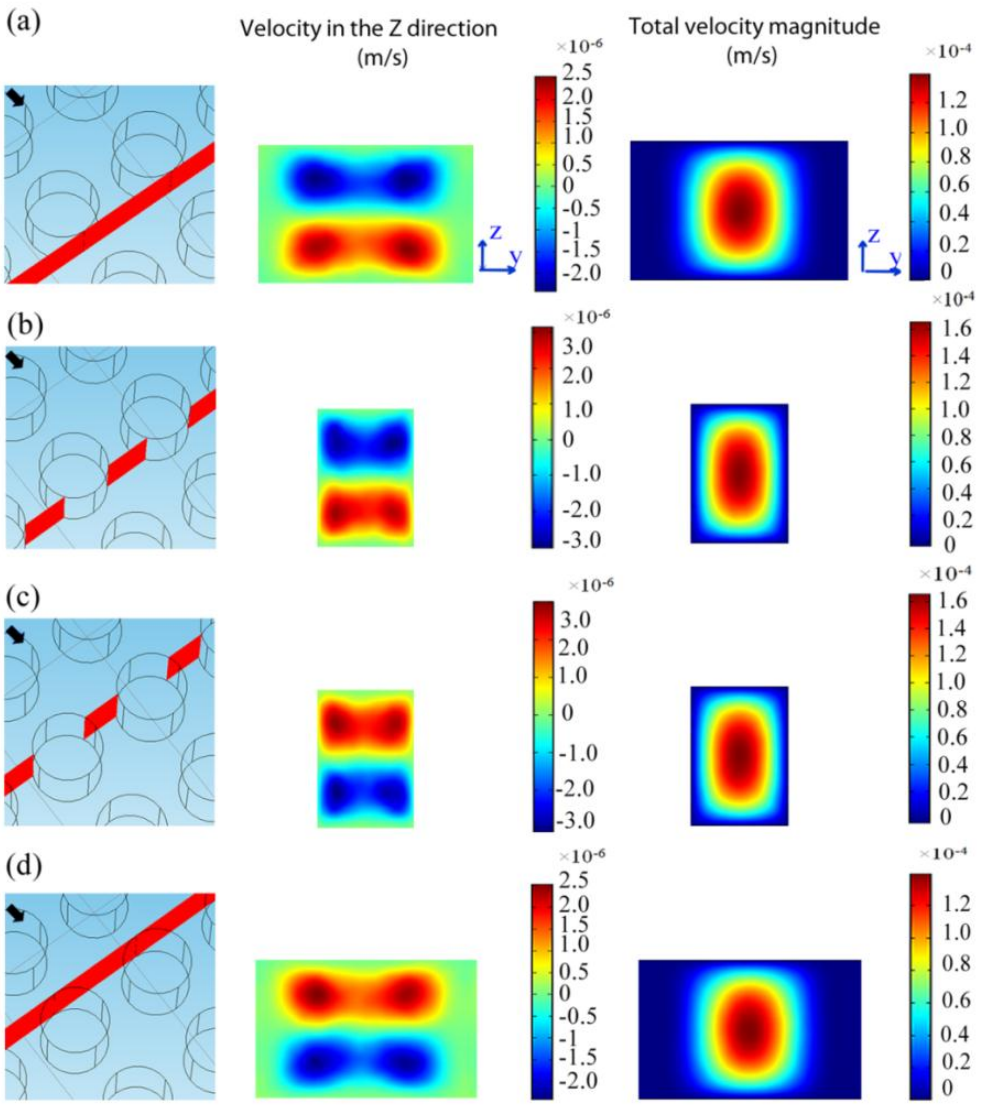

Figure 4.3 Numerical simulation of the *z* component and the total magnitude of the velocity at a *yz* cross section located at (a), (b) 25 µm and 15 µm downstream of a pillar, respectively; and (c), (d) 15 µm and 25 µm upstream of the pillar, respectively. Red and blue colors show the z component of the velocity and have upward and downward directions, respectively (Black arrow shows the direction of the flow.)

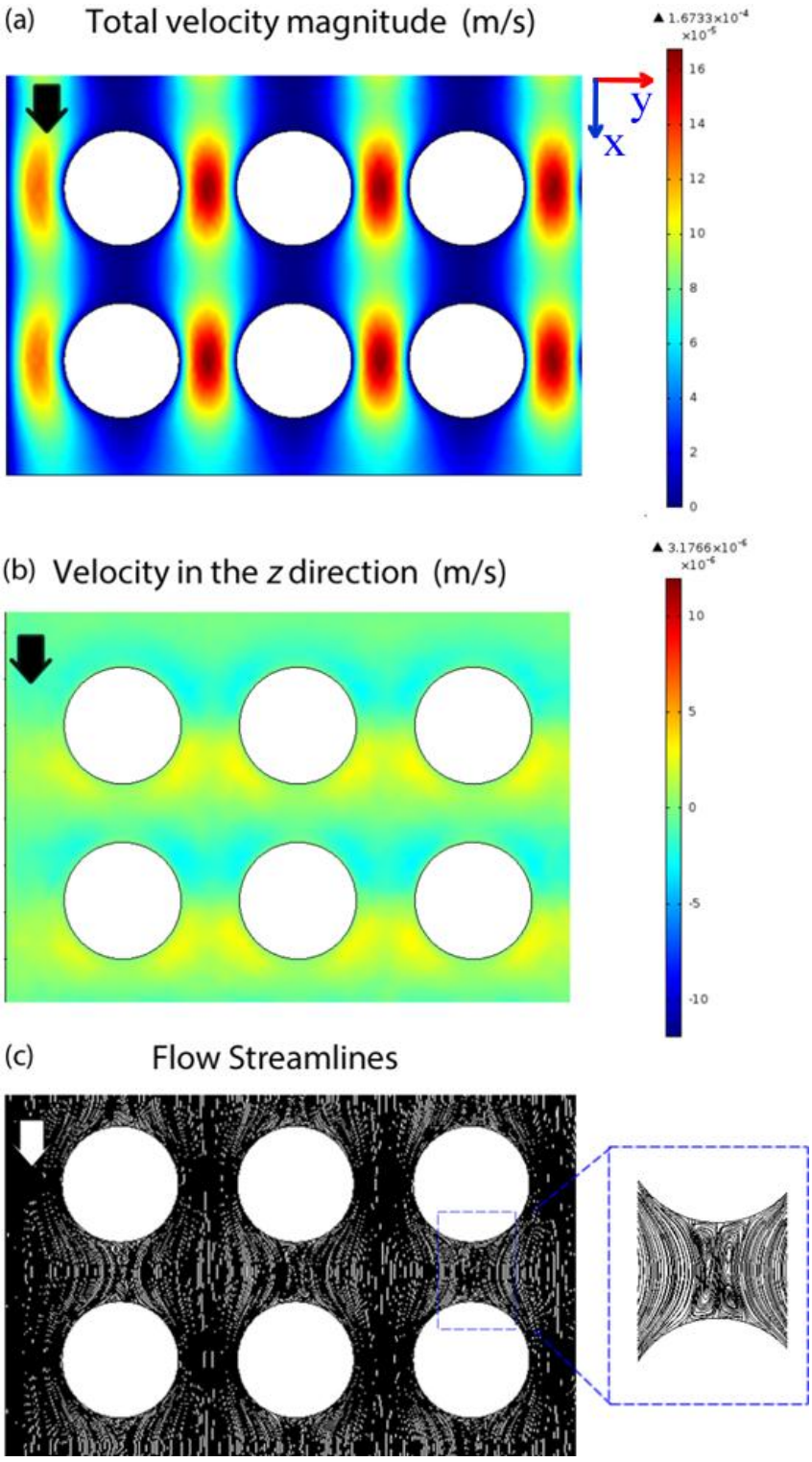

Figure 4.4 Total velocity, *z*-component of the velocity, and flow streamlines for uniform porous pattern at a *xy* plane located at ¼ of height of channel from the bottom surface.

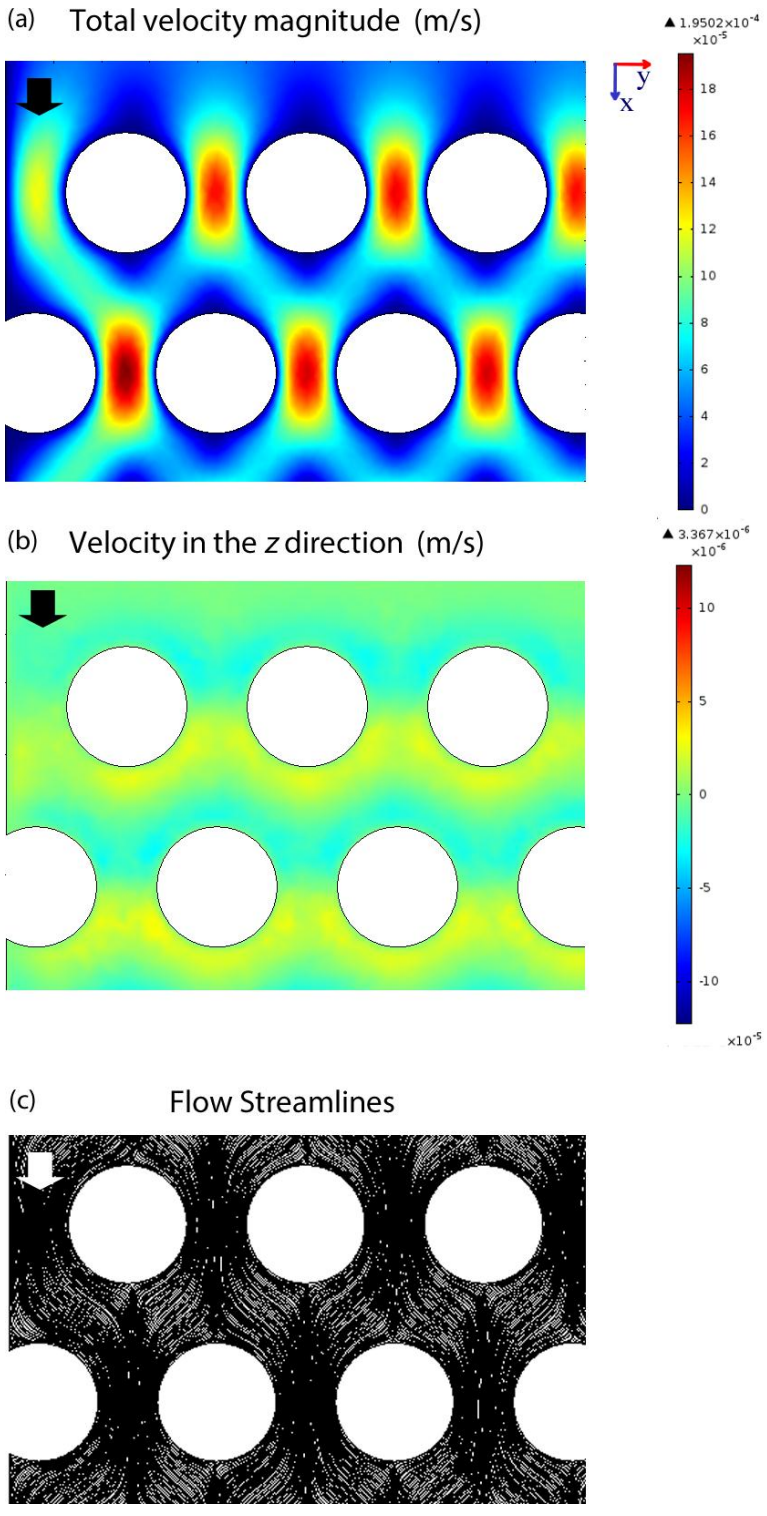

Figure 4.5 Total velocity, *z*-component of the velocity, and flow streamlines for staggered porous pattern at a *xy* plane located at ¼ of height of channel from the bottom surface.

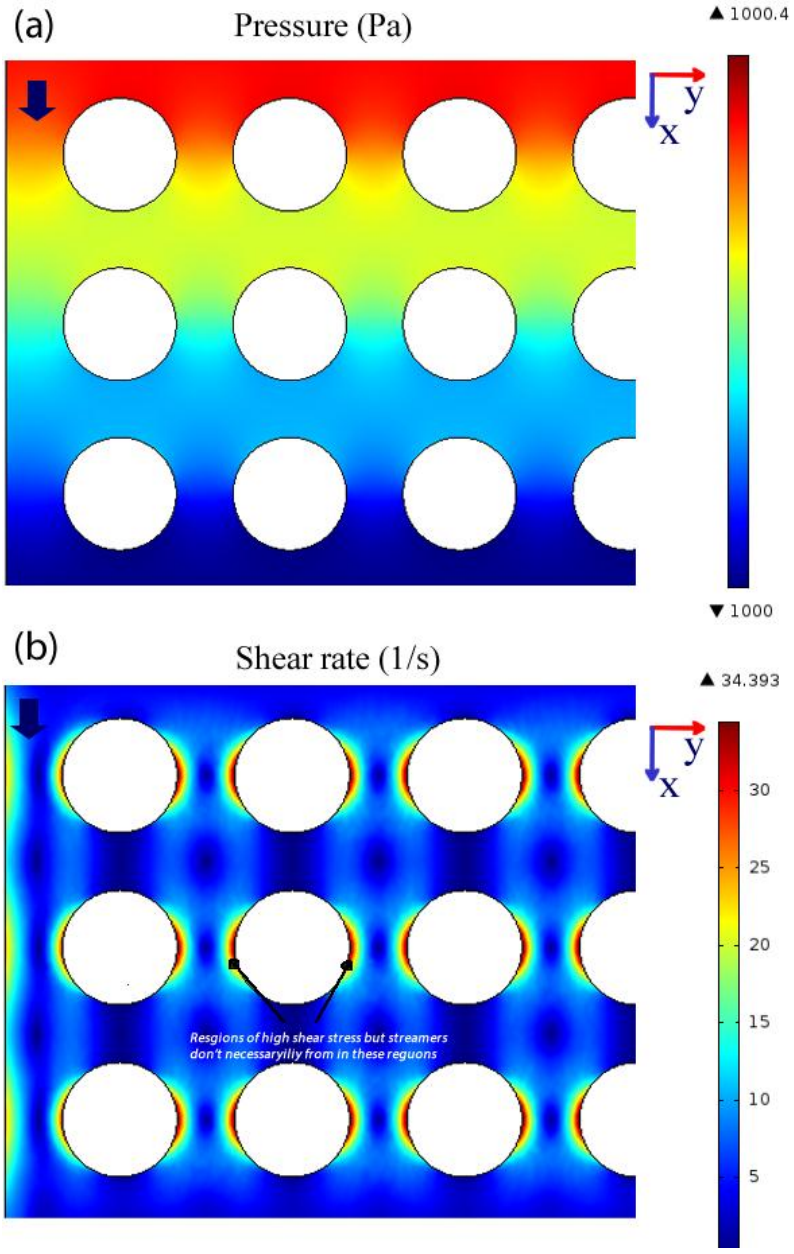

Figure 4.6 Schematic of shear stress and pressure profiles in the device with uniform porous pattern.

4.5 Summary

In this chapter, we presented numerical simulation to study the dynamics of fluid in our microfluidic device. We found the presence of two pair of vortices in the *xy* and *zx* plane in the uniform porous pattern after solving the velocity and pressure fields. However, formation of streamers at different *z*-location demonstrates that the secondary flow in the *yz* plane is an insignificant factor in the formation of streamers. These results stand in contrast with the previous studies which regarded the secondary flow as the underling mechanisms for the formation of streamers in curved channels. Additionally, we found that correlation of streamer with other hydrodynamic parameters such as shear stress and velocity magnitude is not straightforward and further research is required to elucidate the role of hydrodynamic conditions on streamer formation.

5 Summary and future work

This thesis provides a fundamental understanding of the biofilm formation in a porous microfluidic device which consisted of an array of micro posts. We observed that the biofilm structure in our device is mainly consisted of filamentous structures known as streamers and showed that streamer formation is closely related to hydrodynamic conditions. In chapter 2, we explained the microfabrication methods for the fabrication of the microfluidic device and the experimental setup that we used in this study. We used wild type and mutant of *Pseudomonas fluourescens* bacterial strains to form biofilm in our microfluidic device. After the infusion of bacteria for a few hours, we noted the formation of filamentous structures between the micro posts. Some of the important features of the streamer formation such as temporal evolution and spatial organization of streamers under different flow rates were discussed in chapter 3. We observed that the flow rate has an extremely important effect on the formation of streamers. Firstly, we observed that streamer formation occurs within a certain flow range. Additionally, our experiments showed that dynamics of the streamer formation is strongly dependant on the flow rate. In summary, at higher flow rates the onset time for the formation of streamers was decreased, while the number and thickness of the streamers increased at higher flow rate. We also noted the distribution of the streamers across the height of the microchannels. We observed higher number of streamers in the middle of the device at all flow rates. In a few more experiments, we demonstrated that streamer formation is not exclusive to the

pattern of micro-posts and we extended our observations to systems with non-uniform post structure as well as posts of various geometries. In chapter 4, we used fluid dynamical numerical simulation to investigate the interrelationship between the hydrodynamics and streamer formation in more detail and concluded that secondary flows that occur in the vicinity of microposts do not play an important role in the formation of streamers as opposed to the results previously obtained from previous studies on biofilm formation in curved channels.

In future, it is recommended that better microscopic techniques should be used to study the initial stages of streamer formation and elucidate the role of hydrodynamic interactions. Phase contrast microscopes seem to be good candidates for monitoring the streamer formation since they can facilitate the visualization of EPS. Staining the EPS might be another idea to view the development of streamers in the initial stages. Application of different mutants of bacteria that lack some of the organelles such as flagella and pili will be useful in determining their role in streamer formation. In addition, more works can be done on the simulation part of the problem. The model provided here is only an approximation of the real fluidic conditions within porous media. The simulation of the real problem should take into account various factors such as presence of bacteria in the solution and their motility. Additionally, more complex porous media designs could be tested to study the streamer formation phenomena in different industrial applications such as oil recovery and bioremediation. A better understanding of biofilm formation in complex natural

conditions will facilitate not only advancement of fundamental science, but will also benefit various applications.

.

References:

1. Costerton, J.W., et al., *Microbial Biofilms.* Annual Review of Microbiology, 1995. **49**: p. 711-745.
2. Hall-Stoodley, L., J.W. Costerton, and P. Stoodley, *Bacterial biofilms: From the natural environment to infectious diseases.* Nature Reviews Microbiology, 2004. **2**(2): p. 95-108.
3. Stoodley, P., et al., *Biofilms as complex differentiated communities.* Annual Review of Microbiology, 2002. **56**: p. 187-209.
4. *Physiochemical requlation of biofilm formation.*
5. Flemming, H.C. and J. Wingender, *The biofilm matrix.* Nature Reviews Microbiology, 2010. **8**(9): p. 623-633.
6. Shrout, J.D., et al., *The contribution of cell-cell signaling and motility to bacterial biofilm formation.* Mrs Bulletin, 2011. **36**(5): p. 367-373.
7. Battin, T.J., et al., *Contributions of microbial biofilms to ecosystem processes in stream mesocosms.* Nature, 2003. **426**(6965): p. 439-442.
8. Costerton, J.W., et al., *Bacterial Biofilms in Nature and Disease.* Annual Review of Microbiology, 1987. **41**: p. 435-464.
9. Biofilm hypertextbook http://biofilmbook.hypertextbookshop.com/v003/r002/.
10. Mattilasandholm, T. and G. Wirtanen, *Biofilm Formation in the Industry - a Review.* Food Reviews International, 1992. **8**(4): p. 573-603.
11. *Microbial Biofilms: Current Research and Applications*.
12. Logan, B.E. and J.M. Regan, *Electricity-producing bacterial communities in microbial fuel cells.* Trends in Microbiology, 2006. **14**(12): p. 512-518.
13. Kinzler, K., et al., *Bioleaching—a result of interfacial processes caused by extracellular polymeric substances (EPS).* Hydrometallurgy, 2003. **71**(1–2): p. 83-88.
14. Shrout, J.D., et al., *The contribution of cell-cell signaling and motility to bacterial biofilm formation.* MRS Bull MRS Bulletin, 2011. **36**(5): p. 367-373.
15. Cusack, F., et al., *Diagnosis and Removal of Microbial/Fines Plugging in Water Injection Wells*, in *SPE Annual Technical Conference and Exhibition*1987, 1987

Copyright 1987, Society of Petroleum Engineers: Dallas, Texas.
16. Cusack, F., et al., *Field and Laboratory Studies of Microbial/Fines Plugging of Water Injection Wells: Mechanism, Diagnosis and Removal*, 1985, Society of Petroleum Engineers.
17. Blenkinsopp, S.A. and J.W. Costerton, *Understanding Bacterial Biofilms.* Trends in Biotechnology, 1991. **9**(4): p. 138-143.
18. Lennox, J. and J. Ashe, *Biofilms as Biobarriers*. The American Biology Teacher, 2009. **71**(1): p. 20-26.
19. Gerlach, R.C., Alfred B. , *Influence of biofilms on porous media hydrodynamics.*
20. Armstrong, R.T. and D. Wildenschild, *Decoupling the Mechanisms of Microbial Enhanced Oil Recovery,* in *SPE Annual Technical Conference and Exhibition*2011, Society of Petroleum Engineers: Denver, Colorado, USA.
21. Kirisits, M.J. and M.R. Parsek, *Does Pseudomonas aeruginosa use intercellular signalling to build biofilm communities?* Cellular Microbiology, 2006. **8**(12): p. 1841-1849.
22. Stoodley, P., et al., *Flowing biofilms as a transport mechanism for biomass through porous media under laminar and turbulent conditions in a laboratory reactor system.* Biofouling, 2005. **21**(3-4): p. 161-168.
23. Dupin, H.J. and P.L. McCarty, *Mesoscale and microscale observations of biological growth in a silicon pore imaging element.* Environmental Science and Technology, 1999. **33**(8): p. 1230-1236.
24. Dupin, H.J. and P.L. McCarty, *Impact of Colony Morphologies and Disinfection on Biological Clogging in Porous Media.* Environemntal Science and Technology, 2000. **34**: p. 1513-1520.
25. Kim, J.-W., H. Choi, and Y.A. Pachepsky, *Biofilm morphology as related to the porous media clogging.* Water Research, 2010. **44**(4): p. 1193-1201.
26. Whitesides, G.M., *The origins and the future of microfluidics.* Nature, 2006. **442**(7101): p. 368-373.
27. Saleh-Lakha, S. and J.T. Trevors, *Perspective: Microfluidic applications in microbiology.* Journal of Microbiological Methods, 2010. **82**(1): p. 108-111.

28. Squires, T.M. and S.R. Quake, *Microfluidics: Fluid physics at the nanoliter scale.* Reviews of modern physics., 2005. **77**(3): p. 977.
29. Whitesides, G.M. and A.D. Stroock, *Flexible Methods for Microfluidics.* Phys. Today Physics Today, 2001. **54**(6).
30. Gomez, F.A., *Biological applications of microfluidics*2008, Hoboken, N.J.: Wiley-Interscience.
31. Weibel, D.B., W.R. Diluzio, and G.M. Whitesides, *Microfabrication meets microbiology.* Nature reviews. Microbiology, 2007. **5**(3): p. 209-18.
32. Velve-Casquillas, G., et al., *Microfluidic tools for cell biological research.* Nano Today Nano Today, 2010. **5**(1): p. 28-47.
33. Rusconi, R., et al., *Laminar flow around corners triggers the formation of biofilm streamers.* Journal of the Royal Society Interface, 2010. **7**(50): p. 1293-1299.
34. Neethirajan, S., et al., *Biofilms in microfluidic devices*, in *Encyclopedia of Nanotechnology*, B. Bhushan, Editor, Springer: New York.
35. McDonald, J.C., et al., *Fabrication of microfluidic systems in poly(dimethylsiloxane).* Electrophoresis, 2000. **21**(1): p. 27-40.
36. Sia, S.K. and G.M. Whitesides, *Microfluidic devices fabricated in poly(dimethylsiloxane) for biological studies.* Electrophoresis, 2003. **24**(21): p. 3563-76.
37. Yi, C., et al., *Microfluidics technology for manipulation and analysis of biological cells.* Analytica chimica acta., 2006. **560**(1): p. 1.
38. McDonald, J.C. and G.M. Whitesides, *Poly(dimethylsiloxane) as a material for fabricating microfluidic devices.* Accounts of chemical research, 2002. **35**(7): p. 491-9.
39. Cottin, C., H. Bodiguel, and A. Colin, *Drainage in two-dimensional porous media: From capillary fingering to viscous flow.* Physical Review E, 2010. **82**(4).
40. Whitesides, G.M., *Soft lithography.* Abstracts of Papers of the American Chemical Society, 1996. **212**: p. 31-Inor.
41. Zuber, S., et al., *GacS sensor domains pertinent to the regulation of exoproduct formation and to the biocontrol potential of Pseudomonas fluorescens CHA0.* Molecular plant-microbe interactions : MPMI, 2003. **16**(7): p. 634-44.

42. Taylor, S.W. and P.R. Jaffe, *Biofilm growth and the related changes in the physical properties of a porous medium 1. Experimental investigation.* Water Resources Research, 1990. **26:9**: p. 2153-2159.
43. Cunningham, A.B., et al., *Influence of biofilm accumulation on porous media hydrodynamics.* Environmental Science and Technology, 1991. **25:7**: p. 1305-1311.
44. Sharp, R.R., et al., *Observation of thick biofilm accumulation and structure in porous media and corresponding hydrodynamic and mass transfer effects.* Water Science and Technology, 1999. **39**(7): p. 195-201.
45. Hill, D.D. and B.E. Sleep, *Effects of biofilm growth on flow and transport through a glass parallel plate fracture.* Journal of contaminant hydrology., 2002. **56**(3): p. 227.
46. Kim, J.W., H. Choi, and Y.A. Pachepsky, *Biofilm morphology as related to the porous media clogging.* Water Research, 2010. **44**(4): p. 1193-1201.
47. Lim, J., et al., *Nanoscale characterization of Escherichia coli biofilm formed under laminar flow using atomic force microscopy (AFM) and scanning electron microscopy (SEM).* Bull. Korean Chem. Soc. Bulletin of the Korean Chemical Society, 2008. **29**(11): p. 2114-2118.
48. Stewart, T.L. and H.S. Fogler, *Biomass plug development and propagation in porous media.* Biotechnology and bioengineering, 2001. **72**(3): p. 353-63.
49. Nambi, I.M., et al., *Pore-scale analysis of anaerobic halorespiring bacterial growth along the transverse mixing zone of an etched silicon pore network.* Environmental science & technology, 2003. **37**(24): p. 5617-24.
50. Keller, A.A. and M. Auset, *A review of visualization techniques of biocolloid transport processes at the pore scale under saturated and unsaturated conditions.* Advances in Water Resources, 2007. **30**(6–7): p. 1392-1407.
51. Robin, G. and C. Alfred, *Influence of Biofilms on Porous Media Hydrodynamics*, in *Porous Media*2010, CRC Press. p. 173-230.
52. Niederberger, T.D., et al., *Novel sulfur-oxidizing streamers thriving in perennial cold saline springs of the Canadian high Arctic.* Environ Microbiol, 2009. **11**(3): p. 616-29.
53. Reysenbach, A.L., K. Longnecker, and J. Kirshtein, *Novel bacterial and archaeal lineages from an in situ growth chamber deployed at a Mid-Atlantic Ridge hydrothermal*

vent. Applied and environmental microbiology, 2000. **66**(9): p. 3798-806.
54. Hallberg, K.B., et al., *Macroscopic streamer growths in acidic, metal-rich mine waters in north wales consist of novel and remarkably simple bacterial communities.* Applied and environmental microbiology, 2006. **72**(3): p. 2022-30.
55. Van der Kraan, G., et al., *Developmemnt and usage of an etched transparent flowcell for visualization of biofilm induced hetrogenities in porous media using particle image velocimetry.*
56. Paulsen, J.E., E. Oppne, and R. Bakke, *Biofilm morphology in porous media, a study with microscopic and image techniques* Wat. Sci. Tech. . **36**(1): p. 1-9.
57. Kumar, A., et al. *Adhesion and formation of microbial biofilms in complex microfluidic devices*. in *3rd Micro/Nanoscale Heat and Mass Transfer International Conference*. 2012. Atlanta, GA, USA.
58. Thompson, B.W., *Secondary flow in a Hele-Shaw cell.* Journal of Fluid Mechanics, 1968. **31**(02): p. 379-395.
59. BALSA, T.F., *Secondary flow in a Hele-Shaw cell.* Journal of Fluid Mechanics, 1998. **372**: p. 25-44.
60. Taneda, S., *Visualization of Separating Stokes Flows.* J. Phys. Soc. Jpn. Journal of the Physical Society of Japan, 1979. **46**(6): p. 1935-1942.
61. Rusconi, R., et al., *Secondary Flow as a Mechanism for the Formation of Biofilm Streamers.* Biophysical Journal, 2011. **100**(6): p. 1392-1399.

Appendix

Microbiological Experiments

This appendix contains the microbiological protocols that we used in this work. Figure A.1 show the required steps for preparing the inoculums for growing biofilm in microfluidic experiments. The description of each step can be found in the following sections.

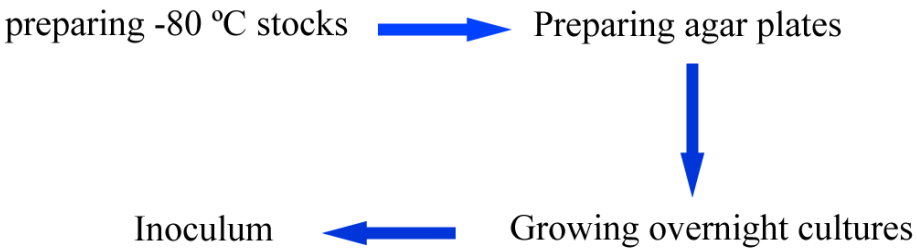

Figure A1. Required steps for preparing inoculums for growing biofilm

1. Preparing -80ºC stocks

Materials:

- ❖ Cryoprotectant material (glycerol)
- ❖ Ultrapure water
- ❖ 2.0 mL screw-cap plastic vials and their container.
- ❖ Agar plates containing *Pseudomonas fluorescens*

Methods:

- Grab a box of screw-cap plastic vials. Add 0.5 mL of ultrapure water. Add 0.5 mL glycerol to the water and replace the cap. Shake the vials and autoclave them.

- Prepare an overnight culture of the bacteria and gently dispense 1 mL of the cell culture to the vials under sterilized biosafety hood.
- Make three copy of each liquid medium and store the vials in a -80 ºC freezer.

2. Preparing agar plates

Materials:

- ❖ LB agar Agar powder
- ❖ Ultrapure water
- ❖ Petri dishes

Methods:

- Add agar powder to the appropriate amount of water (40 gr/L), stir thoroughly and autoclave.
- After autoclaving, wait until the solution cools down. Before the agar solidifies, pour the agar solution in the Petri dishes under biosafety hood. Keep the Petri dishes in their bag in the sterile condition before use. Fill approximately 1/2 of each Petri dish with agar solution.
- Put the lid on the Petri dishes and leave them on a clean and flat bench overnight until the medium hardens. Then place the Petri dishes in the refrigerator upside down.

3. Culturing bacteria on agar plates:

Materials:

- ❖ Agar plates
- ❖ -80 degree stocks of Pseudomonas flurosens
- ❖ Inoculating loop

Methods:

- Place the agar plated and -80 degree stocks of bacteria (or other source of bacteria) under the sterilized the biosafety hood.
- Sterilize the inoculating loop with flame and wait until the loop cools down. Pick the bacteria from the stocks and streak them on the Petri dishes moving in zigzag pattern. Sterlize the loop and spread the bacteria from the previous pattern to a new zigzag pattern. Repeat this process for a few times. Try to lift the lid of the plates as little as possible to avoid contamination.
- Replace the lid and incubate the Petri dishes at 30ºC overnight.
- After the incubation and growth of bacteria, store the Petri dishes in the refrigerator upside down.

Growing overnights cultures for microfluidic experiments:

Materials:

- ❖ LB broth powder
- ❖ Ultrapure water
- ❖ Agar plates contusing *Pseudomonas Fluorosense*
- ❖ 16 mm capped Glass tubes

Methods:

- Dissolve appropriate amount of LB broth powder in water and autoclave the medium
- Transfer 5 ml of the medium in a 16 mm capped tube under the sterilized bio safety hood. Place the Petri dished under the biosafety hood.

- Sterilize the inoculating loop on the flame. Pick a single colony of the bacteria from the agar plated and dip the loop in the solution.
- Replace the cap and incubate the tube in a shaker-incubator at 30ºC overnight (for 16 -18 hours).